Systematic, computational discovery of multicomponent reactions and one-pot sequences.

Rafał Roszak[1], Louis Gadina[2], Agnieszka Wołos[1], Ahmad Makkawi[2], Barbara Mikulak-Klucznik[1], Yasemin Bilgi[2], Karol Molga[1,2], Patrycja Gołębiowska[2], Oskar Popik[2], Tomasz Klucznik[1], Sara Szymkuć[1], Martyna Moskal[1], Sebastian Baś[2,3], Jacek Mlynarski[2] & Bartosz A. Grzybowski[2,4,5]*

[1] Allchemy, Inc., Highland, IN, USA.

[2] Institute of Organic Chemistry, Polish Academy of Sciences, Warsaw, Poland.

[3] Jagiellonian University, Krakow, Poland

[4] Center for Algorithmic and Robotized Synthesis (CARS), Institute for Basic Science (IBS), Ulsan 44919, Republic of Korea.

[5] Department of Chemistry, Ulsan Institute of Science and Technology, UNIST, Ulsan 44919, Republic of Korea.

*Corresponding author. E-mail: nanogrzybowski@gmail.com (B. A. G.).

Discovery of new types of reactions is essential to organic chemistry because it expands the scope of molecular scaffolds that can be made and can help trace new and more economical syntheses of existing structures[1-4]. Within the spectrum of all possible reaction classes, those that build complex scaffolds from multiple simple components in one step (i.e., multicomponent reactions, MCRs[5-11]; Figure 1a) and/or proceed sequentially in one pot[12-14] are appealing as they may capitalize on the use of unstable intermediates, minimize separation and purification operations, and increase the overall step- and atom-economy[15] as well as "greenness"[16,17] of synthesis. However, the number of known MCR classes remains limited to several hundred (Figure 1b and interactive map at https://mcrmap.allchemy.net), and the number of publications reporting new ones appears to decrease in recent years (Figure 1c), perhaps because the most popular reactivity patterns (e.g., isocyanide, β-dicarbonyl, or imine-based MCRs) and their straightforward extensions and combinations[18] have been studied in nearly exhaustive detail. The discovery process continues to rely, per Ivar Ugi's famous quote, on thoughtful "reflection […] or combinatorial techniques,"[5] and even when supported by high-end quantum mechanical methods, requires prior knowledge of "fitting" substrates (e.g., recent ref. [19] vs. closely analogous MCRs from earlier ref. [20,21]). The "reflection" regards not only the choice of substrates but, above all, careful consideration of possible cross-reactivities between numerous intermediates, reagents, and side-/by-products present in a multicomponent mixture – in effect, translating into a laborious analysis of complex networks of mechanistic steps. Here, we show that computers equipped with accurate and broad knowledge of mechanistic transforms can perform such network analyses rapidly and in a high-throughput manner, and can guide systematic discovery, ranking, and yield estimation of unprecedented types of MCRs, one-pot sequences

and even organocatalytic reactions, several of which we validate by experiment. These results evidence that synthesis-planning algorithms are no longer limited to skillful manipulation of the existing knowledge-base of "full reactions"[22-28] but can assist in its creative expansion.

Every chemical reaction is a sequence of elementary steps or, at a less precise but very popular representation of arrow-pushing steps[29], which has been used in computational chemistry for decades[30-35] (though in most cases to analyze only certain types of chemistries and with limited accuracy, see Supplementary Section S6 in ref. [40] and **Section S3** here). This level of description is appealing because, compared to quantum methods, it reduces the number of degrees of freedom one needs to consider, while still retaining enough accuracy to rationalize the mechanisms of the vast majority of organic chemical transformations, including the newly discovered reactions[1,2,36,37]. Here, we use a large and diverse set of arrow-pushing "operators" to generate networks of mechanistic steps starting from sets of multiple substrates/components potentially exhibiting different modes of reactivity. We then aim to identify the mechanistic pathways and conditions that would select only some of these modes and would proceed, in one pot, cleanly into products significantly more complex than the starting materials. Uniquely and mindful of various cross-reactivities possible in multicomponent reaction mixtures, we consider possible by-products, products of side reactions, products of reactions between these by- and side-products, and analyze potential interference of all these species with the "main" mechanistic pathway. We scrutinize these processes for kinetics to ensure that side-processes do not hijack the desired sequence, lowering or even nullifying its yield, which we also aim to approximate. Within this general approach, the problem of designing MCRs or one-pot sequences becomes one of selecting the substrates, expanding the mechanistic networks "forward" and "sideways" from these substrates, and performing kinetic analysis to trace conflict-free mechanistic routes (**Figure 2**).

Algorithmic details.

Choice of substrates. While the algorithm accepts any user-specified molecules as input, "guessing" the substrates resulting in productive MCRs may be challenging and, instead, we rely on a high-throughput analyses of substrate combinations from a house-curated collection of diverse and commercially available small molecules featuring one or two groups reactive in various types of transformations (**Figure 2a** and, for details, **Methods** and Supplementary **Section S4**). This collection comprises 2200 molecules and offers billions of choices of substrate triplets and/or quartets, which we survey systematically as described later in the text.

Mechanistic transforms. Because no adequately diverse databases of *generalized* (beyond specific literature precedents, cf. **Methods**) templates describing mechanistic steps are publically available, we expert-coded in the SMARTS notation[38,39] a collection of ~8000 commonly accepted (i.e., already known rather than some hypothetical ones) mechanistic transforms, roughly at the aforementioned "arrow-pushing" level. This collection includes a broad range of chemistries although it is certainly not yet exhaustive (**Methods**). Transforms are categorized according to typical reaction conditions, temperature range and water tolerance, typical speeds (very slow, slow, fast, very fast, and unknown if conflicting literature data have been reported, VS-S-F-VF-U). They provide suggestions for commonly used reagents and delineate the scope of admissible groups. Importantly, unlike in our prior works on complete reactions[22,23,25-27,39] or carbocationic rearrangements[40], each mechanistic transform is coded to account for by-products (**Figure 2b**) – this is essential for the aforementioned "sideways" analyses of mechanistic networks. Since the focus of the algorithm is to generate new scaffolds, the algorithm does not consider stereochemistry. For more details, see **Methods** and User Manual in Supplementary **Section S1**.

"Forward" expansion of mechanistic networks. For a given set of substrates (henceforth, synthetic generation G_0), the algorithm applies the mechanistic transforms to create the first-generation, G_1, of products and by-products, which are then iteratively reacted[23,25] to give generations G_2, G_3 (up to some user-specified generation n), resulting in rapidly expanding[26] networks of mechanistic steps (**Figures 2c,3a**). At this stage, all classes of reaction conditions are allowed to survey the "synthesizable space" broadly. Within this scheme, if a given substrate can engage in a very-fast, VF, step (e.g., tautomerization, elimination leading to an aromatic product, intramolecular proton transfer, etc.), only this rapid step is performed under given reaction conditions; other competing mechanistic steps can be applied to this substrate only if they proceed under different conditions. For instance, a substrate like 2,4-cyclohexadienone under basic conditions will not be allowed to undergo a hypothetical CH-deprotonation and subsequent alkylation reaction, as it is certain that a tautomerization to aromatic phenol will occur much faster. Moreover, intermediates containing highly strained scaffolds not known as reaction intermediates (e.g., cyclobutenylene but not benzyne) are eliminated. Molecules can also be checked for the pKa of all C-H bonds[41] to ensure that reactions with electrophiles, such as C-H alkylations, proceed at the most acidic positions. Also, to prevent oligo/polymerization and limit network's size, each substrate is allowed to contribute atoms to any molecule in the network at most twice (see User Manual).

Selection of mutually-compatible MCR/one-pot sequences. Pathways leading to every neutral molecule within the network thus created are traced by Dijkstra-type algorithm; if multiple routes are detected, they are retrieved and ranked according to length. For any of these mechanistic sequences to be suitable candidates for MCR or one-pot reactions, the conditions specified for

individual mechanistic steps must be "matching". This is the "Level 1" of analysis (**Figures 2c**, **3a**) and the sequences:

(i) Cannot combine steps requiring oxidative and reductive conditions, and cannot use water-sensitive steps after water-requiring ones;

(ii) Should use solvents of the same class, although protic solvents are allowed to be added to aprotic ones (but not vice versa);

(iii) Cannot change multiple times between non-overlapping high and low temperature ranges (which would be experimentally impractical);

(iv) Should allow only for "monotonic" changes in acidity (e.g., basic-acidic-basic changes are not allowed). Additionally, steps proceeding in strongly basic conditions (with, e.g. LDA) are not allowed if earlier steps required acidic conditions.

Sideways network expansion around "main" MCR/one-pot routes. If Level 1 analysis identifies a candidate, conditition-matching sequence, the aforementioned "sideways" analysis of potential side reactions is performed (**Figure 2d**, **3b**). At Level 2, the kinetics of side reactions are examined. Initially, this is done in a rudimentary manner, according to the aforementioned "very slow-slow-fast-very fast-uncertain" categorization of reaction steps (cf. examples in **Methods**). In particular, warnings are assigned if, for a given reaction of the main path, a side-step possible under the same or similar conditions is faster (for obvious reasons, such comparisons are not made on the "uncertain" reactions). Such cases are flagged but not permanently removed from the mechanistic network since it is sometimes possible to generate thermodynamic products via a slower reaction (e.g., slow 1,4-addition of cyanide to methyl-vinyl ketone vs fast 1,2-addition). Additional warnings are assigned if any of the by-products shows cross-reactivity with the main

pathway or the reaction mixture becomes too complex (e.g., if three or more metals from catalysts or reagents are present and there is a possibility for unforeseen complexation of active species or deactivation of catalysts by ligand exchange). The by- and side-products from Levels 1 and 2 are allowed to react further, to give species at expansion higher Levels, for which similar cross-reactivity analyses are performed. Importantly, the algorithm also analyzes whether reactivity conflicts between forming intermediates and yet unreacted substrates exist. If all substrates contributing atoms to the final product can be present in the reaction vessel from the beginning, the sequence is categorized as a plausible MCR (with possible condition changes obeying (i)-(iv) above); if, however, some intermediates are found to be cross-reactive with the substrates, then the algorithm suggests a one-pot option with sequential addition of the problematic substrate. In the current work, we focus on MCRs and one-pot sequences that entail no unresolved conflicts or warnings within Level 4 networks (see realistic examples in **Figure 3b** and **Extended Figures 1-5**). Such networks can be propagated, for arbitrary substrates, within the MECH module of the Allchemy platform[23,25,40] which is available to academic users at https://mech.allchemy.net.

Prioritization and post-design evaluation. Because even for small substrate sets, the networks thus constructed may span large numbers of plausible MCR/one-pot products (**Figure 3a**), additional analyses are performed to identify those that offer maximal complexification of the scaffold, those producing previously unknown scaffolds, those that are similar to approved drugs, and more (see **Methods**). The algorithm can also read in the positions of experimentally recorded mass-spectrometric signals and map them onto the L2-L4 networks, which often facilitates analysis of experimental reaction mixtures (cf. **Figure 3b** and **Extended Figure 1**; also User Manual in Supplementary **Section S1**).

Estimation of yields. Finally, once a desired MCR/one-pot candidate is selected, the algorithm performs a more in-depth kinetic analysis aimed at the estimation of reaction's yield. Since experimental kinetic rate constants for the vast majority of mechanistic steps are not available, we developed a physical-organic model grounded in free-energy linear relationships and approximating the rate constants of mechanistic steps using Mayr's nucleophilicity indices (see [42,43] and **Methods**).

Overall, for small substrate sets (3-5 starting materials), the entire procedure from the generation of the main network to yield estimation for MCR candidate(s), typically takes few minutes on a multicore desktop machine. Reassuringly, when appropriate substrates are input, the algorithm uses it mechanistic knowledge to "re-create" the known MCRs (e.g., Mannich 3CR, Passerini 3CR, Petasis 3CR, Ugi 4CR, etc.). More interestingly, for many other substrate combinations, it finds unprecedented sequences to which we now turn.

Experimental validations.

From amongst the multitude of putative MCRs the algorithm has thus far identified, we scrutinized in detail several hundred and committed to synthesis ten: three one-pot sequences, five MCRs, and two substrate-regenerating or organocatalytic reactions. In selecting these examples, we were guided by the mechanistic novelty, substrate-to-product complexity increase, and/or potential usefulness of the scaffolds produced. Another factor was the conciseness of these protocols vs. traditional retrosynthetic planning that is based on "full reactions" rather than mechanistic steps and cannot capitalize on the use of reactive intermediates. Accordingly, for all one-pot/MCR products we also ran the state-of-the-art retrosynthestic program (Chematica/Synthia[22-24]) which either planned multistep routes (all deposited at https://zenodo.org/records/10817102; on average 4 and up to 11 steps) or did not suggest any

syntheses at all. All sequences are named "Mach" to highlight their machine-driven discovery (and to allude to its speed).

One-pot, non-MCR sequences. We begin with a sequence that is, admittedly, simple but serves to illustrate various modalities of the algorithm. Starting from enone, alkyllithium, azidohalide and alkyne – selected because they contain multiple nucleophilic and electrophilic sites and are thus likely to generate a multitude of scaffolds – the mechanistic network propagated to the fourth generation, G_4 (**Figure 3a** and https://mcrchampionship.allchemy.net for interactive version) contained conditions-matched sequences leading to as many as 391 products with MW < 500. This analysis revealed two scaffolds in G_4 that stand out because they correspond to previously unreported (*green* node interior), tricyclic scaffolds with large per-step complexity increase from the substrates (*large* node size, see **Methods**), and because the scaffold produced via the *blue* route features a spiro system akin to that in some drugs and bioactive agents[44-47]. The mechanistic sequences to these scaffolds diverge at the initial step. The Mach1 route traced in *blue* proceeds via the 1,2 addition, generation of the alkoxide intermediate, *O*-alkylation, and click reaction closing two rings. The Mach2 *orange* route starts with 1,4, Michael-type addition creating a carbanion at the alpha carbon, followed by *C*-alkylation and click reaction. Moreover, the algorithm predicts that (1) in order to avoid a reactivity conflict during metalation of alkyne (marked in *pink* in the L4 view in **Figure 3b**) , the sequence may be performed only as one-pot rather than MCR (with enone added only after the complete consumption of the alkyllithium substrate); (2) the initial steps in both routes can be carried out using propargyllithium, with HMPA acting as a "switch" (**Figure 3c**) to promote the 1,4 addition[48]; and (3) that both sequences will result in poor yields, ca. 20-40%.

All these predictions turned out correct. When both sequences were carried out under computer-suggested conditions (fine-tuned for triflate vs. bromide/iodide leaving group in the haloazide substrate, **Figure 3c**), the isolated yields of different derivatives shown in **Figure 3d** ranged from 12 to 44%. Of note, the computer-predicted competing reactivity modes were also congruent with ESI-MS analyses – in **Figure 3b** and **Extended Figure 1**, larger *orange* nodes denote side-/by-products with masses matching the spectra.

Another prediction for a one-pot, Mach3 sequence relying on a 2,3-Wittig rearrangement and leading to branched a diallylic ethers, is illustrated in **Figure 4a** and further detailed in **Extended Figure 2**. This sequence was committed to experiment validation because, after metathesis (not compatible with one-pot conditions and carried out separately, dashed reaction arrow in **Figure 3a**), it affords access to cyclic enol ether scaffolds that are used in various medicinal syntheses[49-52]. The algorithm predicted that this sequence would proceed in good, ~68% yield and, indeed, the yields for derivatives shown in **Figure 4b** were 66-96%.

MCR sequences. Turning to MCRs rather than one-pot sequences, **Figure 4c** illustrates a Mach4 reaction (from L1 and L4 networks illustrated in **Extended Figure 3a**), in which an allene, a maleimide derivative, and a carboxylic acid anhydride engage in a sequence of Claisen rearrangement, aromatization, Diels-Alder cycloaddition, deprotonation and acylation to yield a 1-(1-cyclohexenyl)naphthalene, atropisomeric scaffold familiar from various types of drugs (e.g., refs [53,54]). Scaffolds of this type are typically prepared via metal-catalyzed couplings between naphthalene derivatives with vinyl partners[55,56], activation of the aryl C-H bond with a Co-catalyst and an imine as a directing group[57], or annulation of arynes with alkynes using either Pt catalysts[58] or halogen electrophiles[59]. The MCR approach shortens these procedures while commencing from substrates of similar complexity (allene is prepared readily in two steps from commercially

available 2,3-butadien-1-ol) and does not require transition metal catalysts or pre-functionalized aryl systems. For the parent compound in **Figure 4c** and its analogues obtained using different dienophiles in **Figure 4d**, the experimental yields were generally quite satisfactory and in most cases >90% (for the originally predicted sequence, the algorithm predicted 99% vs. 96% in experiment).

Another pair of MCRs using allene as one of the substrates is illustrated in **Figure 4e** and begins with a nucleophilic addition of an allyl thiol to the allene and isomerization followed by thio-Claisen rearrangement. Interestingly, at this point, network analysis detailed in **Extended Figures 4** and **5** indicates that the sequence can diverge. In Mach5 MCR, addition of excess base results in straightforward condensation with an aromatic aldehyde occurring at the less acidic methylene group of the thioketone. By contrast, in Mach6, addition of acetyl chloride triggers a relatively rare[60] sequence of acetylation of alcohol, acidic elimination of acetic acid catalyzed by the in-situ generated HCl to give the Knoevenagel-type adduct, thioketo-enol tautomerization followed by spontaneous cyclization to give a product containing a 2,3-dihydrothiophene moiety. The product of the first, as-predicted MCR is obtained in 57% yield (vs. predicted 43%) with further derivatives prepared with the same methodology shown in **Figure 4f**. This MCR is interesting insofar as such scaffolds can further react with phenyl hydrazine[61] to give substituted pyrazoles which are popular motifs of many drugs (this reaction is not compatible with the MCR conditions and we carried it out separately in 53% yield; dashed arrow in **Figure 4e**). The 2,3-dihydrothiophene products are obtained in significantly lower yields (~10% and up to 14% for the cyano derivative vs. 12% predicted yield, though these experimental values are affected by partial decomposition of the product during purification), and their applications are less conspicuous[62].

The sequence underlying Mach7 MCR shown in **Figure 4g** – leading to a scaffold akin to oblongolide natural products considered as potential algicide, herbicide[63] and antiviral[64] agents – is perhaps familiar to a retrosynthetically-trained eye. Indeed, the succession of transesterification of sorbic alcohol, Knoevenagel condensation and Diels-Alder reaction has also been predicted by Chematica/Synthia. Our main interest in this sequence was whether the algorithm was correct in predicting that it could be folded-up into a one-step MCR. The results for the original sequence in **Figure 4g** and derivatives in **Figure 4h** verified that it could, with yields of racemic mixture up to 59% (compared to 55% predicted by the algorithm and 13-38% for multistep syntheses of similar scaffolds reported in [65,66]) and with the procedure readily scalable to gram scale (Supplementary **Section S5.7**). Diastereocontrol derives from the Knoevenagel condensation yielding selectively *Z*-benzylidenes, and the intramolecular Diels-Alder reaction is moderately sensitive to the substitution of the aldehyde used but very sensitive to the exchange of alcohol's methyl by phenyl. Also, one less obvious outcome predicted by the algorithm is that for the indole-3-carbaldehyde substrate, the Knoevenagel adduct can engage in a reverse-demand Diels-Alder cycloaddition to give a relatively complex, tetracyclic scaffold marked with a star in **Figure 4h** and isolated in 24% yield.

Substrate-reusing and organocatalytic sequences. The last two examples are interesting for the unique ways in which they use or *reuse* some of the substrates. In the Mach8 sequence shown in **Figures 5a,b**, the phenol substrate is first used to form an activated ester that then reacts with 2-allylcyclohexanone to give a spiro β-lactone which, upon addition of $MgBr_2$, undergoes a ring-expanding rearrangement into a substituted hexahydro-2(3H)-benzofuranone in 31% yield (vs. predicted 48%). Such motifs are found in various natural products and bioactive compounds[67] and the particular scaffold, upon metathesis and reduction, could create a ring system present in

lancifonins. However, when iodo-substituted phenols and cyclohexanone (instead 2-allylcyclohexanone) are used as substrates, and when network is propagated to higher generations, the continued pathway (Mach9, shown in the bottom part of the figure) appears interesting, as the iodophenol is first used as above, then becomes a by-product of the spirocyclization step and then – when the product decarboxylates at elevated temperature – is *reused in situ* as a substrate in Heck reaction (upon addition of Pd catalyst). Ultimately, this use-release-reuse sequence proceeds in 35% yield (vs. predicted 35%) which is appreciable given that it spans 10 mechanistic steps (and a separate, final transformation into acetyl esters to facilitate separation of products).

Finally, **Figures 5c-e** illustrate a Mach10 reaction that was predicted and then confirmed as organocatalytic. With the initial set of substrates (α-bromo-α,β-unsaturated ester, methyl thioglycolate and sodium azide), the algorithm suggested an MCR that could lead to a dihydrothiophenecarboxylate scaffold similar to some GABA receptor inactivators[68]. However, the program also indicated that that the C-H pKa of the α-azidoester was higher than that of the α-thioester – that is, the deprotonation (either by azide anion[69] or sodium methoxide) at the former locus was preferred and could lead to elimination (*green* arrow in **Figure 5c**, *blue* arc connection in the L2 network in **Figure 5d**) rather than cyclization. Because elimination is rapid (as is recognized as such by the algorithm) and regenerates the deprotonated thiol substrate (*pink* in **Figure 5d**), we expected that the "cycle" could be sustained and the thiol could act as an organocatalyst, effectively translating into a previously unknown organocatalytic azide substitution at vinylic α-position. This was, indeed, verified in experiment with the original reaction proceeding under mild conditions in 67% yield (vs. algorithm-predicted 47%), and with the further scope illustrated in **Figure 4e**. For alkyl ketones, 10 mol% of the thiol is optimal, while for β-aryl ketones, 35 mol%

thiol load is necessary due to the trapping of the thiol catalyst in the S_N2 reaction with the alkyl bromide (obtained after 1,4-addition of thiol to Michael acceptor).

Discovery automation and MCR Championships.

The above examples are but a tiny fraction of substrate combinations that can give rise to MCR or one-pot sequences. To speed up the discovery process, we have automated the choices of substrates (from the aforementioned set of 2200 reactive molecules, cf. **Methods**). In this procedure, different triples and quartets of substrates are systematically scanned, networks are propagated to G_9 and analyzed to L4 and top-scoring (according to complexity increase per step metric, $\Delta C/n$, see **Figure 1** and **Methods**) and warning-free candidates for MCRs and one-pots are retained. With mechanistic networks originating from tens of thousands of substrate combinations now tested, and with further searches ongoing, the list of the currently 50 top-ranked MCR candidates is maintained at https://mcrchampionship.allchemy.net. Users of Allchemy's MECH (https://mech.allchemy.net) can perform searches with their own substrates of choice, and can opt to "compete" and post their results therein (if the scores place them within top-50), in the world' first "championship" for computerized reaction discovery.

Conclusions and Outlook.

Although it can certainly be argued that at least some MCR/one-pot reactions we described could have been "spotted" by trained human experts, computers help systematize and accelerate the discovery process manifolds – in the fullness of time, in quantities that may have significant impact on the practice of synthetic chemistry. In our own experience, MECH has proven to be a very effective "idea generator" and, in conjunction with MS, very helpful in explaining compositions of reaction mixtures and guiding structural assignments of complex yet unexpected products (these aspects will be published separately). This said, algorithms like ours do not replace

all of chemists' insights (e.g., in terms of fine-tuning exact temperatures, specific solvents, etc.) and certainly have room for further improvement (see **Extended Figure 6**, for an example of incorrect MCR prediction). Looking forward, we aim to (i) further extend the 8000 rule set, notably to incorporate radical-based steps (cf. **Methods**); (ii) adapt the MECH algorithm to the "retro" direction (to suggest imaginative disconnections of specific scaffolds) and, most ambitiously, (ii) to investigate whether our collection of mechanistic transforms could be used in conjunction with generative AI to discover completely new mechanistic steps.

Methods.

Mechanistic rules. As outlined in the main text, the mechanistic transforms are encoded in the SMARTS notation and account for by-products. The templates are generalized – that is, they do not encompass just a single reaction precedent (as in the recently published repository of mechanistic steps for popular radicalic reactions[70]) but each specifies the scope of admissible substituents at various positions of the SMARTS template as well as a list of incompatible groups. These explicitly defined incompatibilities help limit the sizes of the networks and remove from analysis at least the obviously problematic steps, in which two or more motifs would react on commensurate time scales, inevitably leading to undesired complex reaction mixtures and ruining a "clean" MCR. In Allchemy's MECH module, the user can choose to treat incompatibilities either restrictively (with ~1200 groups considered as potentially conflicting during mechanistic transforms' coding and with each transform assigned, on average, 133 such groups) or permissively (considering only ~50 most common groups and with, on average, 26 assigned per transform). The current work uses the conservative approach but the permissive one can also be useful in generating more adventurous ideas (albeit at the expense of more false-positive predictions).

Furthermore, rules are accompanied by information about reaction conditions that is essential to later "wire-up" individual mechanistic steps into mutually compatible sequences. In this context, each transform is categorized according to general conditions (basic, neural, acidic), solvent class (protic/aprotic and polar/non-polar), temperature range (very low = < -20 °C, low = -20 to 20 °C, r.t., high = 40 to 150 °C, and very high = > 150 °C); and water tolerance (yes, no, water is required). One transform can have more than one categorization (e.g., Diels-Alder cycloaddition can be carried out either under neutral conditions at high temperature or at very low,

low or room temperatures using a Lewis acid catalyst) – in such cases, multiple conditions are provided and, when considering sequences of compatible steps, are treated as logical alternatives. Each transform also contains specific suggestions for reagents commonly used in reactions involving this mechanistic step (e.g., diethylaluminium chloride in Claisen rearrangement, *n*-butyllithium in [2,3]-Wittig rearrangement, etc.).

Regarding the initial and rough categorization of kinetics, each transform is assigned a typical speed category (very slow, slow, fast, very fast, uncertain). A "very slow" step (conversion time above ca. 24 hrs) is, for example, addition of amines to trisubstituted Michael acceptors. Steps categorized as "slow" (few to ca. 24 hrs) are, e.g., reaction of a deprotonated nitro compound with a ketone, addition of an alcohol to a protonated nitrile, or 1,3-dipolar cycloaddition of imine and nitrile oxide. Examples of "fast" steps (minutes to few hrs) include deprotonation of alcohols, alcoholysis of anhydrides, or addition of organocuprates to activated alkenes. "Very fast" steps (seconds to minutes) are, for example, decomposition of oxaphosphetanes to alkenes and phosphine oxide, elimination of a chloride anion from an adduct of amine and acyl chloride, tautomerizations leading to aromatic compounds (e.g., 2,4-cyclohexadienone to phenol). "Uncertain" steps are those for which literature provides conflicting reaction data (i.e., wide range of reaction times and/or rates strongly influenced by substrate structures or small changes in reaction conditions) or those for which literature is insufficient to determine the reaction rate of an individual mechanistic step. One example from this category is addition of an imine to phenolic compounds, for which reaction rate strongly depends on the activity/nucleophilicity of phenolic component but even more on reaction conditions, resulting in time spans from 5 minutes to 9 hours for reactions involving the same substrates (see ref. [71] – 9h; [72] – 7.5h; [73] – 3h; [74] – 5 minutes]). Another example is S_N2 reaction of a secondary bromide with cyanide anion, for which the reaction

rate is strongly influenced by the character and size of substituents on the halide component and the type of solvent used, with polar aprotic solvents facilitating the reaction and polar protic solvents impeding it. For instance, reaction of 2-bromo-2-(2-methylphenyl)-1-(morpholin-4-yl)ethanone with sodium cyanide in methanol takes 24 hrs[75], while reaction of a similar molecule, methyl 2-(1-bromo-2-methoxy-2-oxoethyl)benzoate, with potassium cyanide in DMF takes only 1 hr[76]).

The rules covered in the current version of the MECH module span a broad range of acid-base catalyzed steps (including Lewis acids), substitutions, eliminations, additions, rearrangements, pericyclic reactions as well as basic transformations catalysed by transition metals (e.g., mechanistic steps of Suzuki, Buchwald-Hartwig, Heck, and Pauson-Khand reactions). Basic carbocationic chemistry is included but not exhaustively (a separate HopCat module dedicated to such rearrangements is available in our recent publication[40]). Also, radical mechanistic steps are not (yet) included since their proper application requires generalization (cf. short discussion in Supplementary **Section S3** illustrating the pitfalls of encoding precedent-based mechanistic steps[71]) and likely additional heuristics based on thermodynamic and molecular-mechanical considerations (akin to those we described in the HopCat paper[40]). Some rare types of steps involving π-complexes had to be simplified in notation since they are not properly handled by RDKit (they are encoded as 3-membered rings rather than interaction between metal and multiple bonds, e.g., during Heck reaction).

Additional details of network expansion. During expansion of mechanistic networks, the program generally uses the individual steps, e.g., imine formation is divided into 1) ketone protonation, 2) imine addition to the protonated ketone, 3) proton transfer from nitrogen to oxygen, 4) formation of an iminium cation via elimination of water, 5) deprotonation of the iminium cation

(**Extended Figure 7a**). However, because the networks expand very rapidly with the number of steps ("synthetic generations"), such step-by-step expansions may be inefficient in exploring longer mechanistic sequences – for instance, the five-step imine formation is only part of, say, the Ugi multicomponent reaction. To reduce computational cost, we have also encoded some "shortcut" steps that, for popular transformation types, concatenate individual mechanistic steps (those occurring in a rapid sequence and/or those leading to unstable intermediates; see example in **Extended Figure 7b**). When executed as one "super-step", the shortcuts keep all the information about by-products of all individual steps. The network expansions then use both the step-by-step and shortcut strategies.

Further details of route prioritization and post-design evaluation. The MECH module offers multiple options to filter, analyze, and prioritize the one-pot/MCR pathways within the mechanistic networks. As described in detail in Supplementary **Section S1**, the user can filter off those products that are formed via mechanistic steps having non-overlapping "cores" (reactions occurring on disjoint parts of the molecule will likely yield "linear" structures and will not complexify the starting scaffold), or those that do not involve any rearrangements or pericyclic reactions.

To easier identify and prioritize sequences that offer the highest degree of complexification, nodes in the network can be sized in proportion to the increase of structural complexity per step, $\Delta C/n$, where ΔC is calculated along an atom-mapped path as $(a \cdot \#Rearrangements + a \cdot \#RingsFormed + \#BondsCreated + \#BondsDisconnected)$, where $a = 5$ is used here to strongly favor formation of cyclic scaffolds and sequences containing rearrangements. Furthermore, the nodes can be colored as molecules known/unknown in the literature or, more generally, according to whether the scaffold is unprecedented. The algorithm to determine scaffold

novelty first defines a scaffold "base" as a set of connected rings, whereby a ring is considered "connected" if it fulfills either of the two criteria: a) it shares at least one atom with any of the other rings in the base, b) is connected with a double bond to any of the other rings. The final scaffold is obtained from this "base" by inclusion of atoms connected to the base with double bond (i.e., oxygen from carbonyl group or exomethylene double bond). Note that this definition inherits both elements and bond orders from the parent molecule such that, for instance, cyclohexane, cyclohexene, cyclohexanone and cyclohexanethione are all considered as different scaffolds. Finally, a scaffold is considered novel if it is not present in the list of 95 191 scaffolds extracted from the Zinc collection[77]. The nodes within the networks can also be colored by similarity to approved drugs, reaction type, hazardous compounds, and more (see User Manual in Supplementary **Section S1**). Last but not least, the user can input a list of mass-spectrometric signals recorded in experiment and the likely M+1 and M+23 nodes will be marked on L1-L4 trees (**Figures 2b** and **Extended Figure 1**).

Estimation of yields. To estimate the yields of MCR/one-pot candidates, we developed a physical-organic model grounded in free-energy linear relationships. In this model, to be detailed in a separate publication, the rate constants of mechanistic steps are approximated by using Mayr's nucleophilicity, *N*, and electrophilicity, *E*, indices[42,43] as $logk_{20deg} \sim (N + E)$, which are further fine-tuned by corrections capturing relative reactivities, stoichiometries and amounts of various species in the mechanistic networks, $logk_i = log\ k_i^{Mayr} + \sum corrections(r_i)$. The weights of the individual corrections were trained on the mechanistic networks of 20 diverse MCRs reported before (chosen to represent both low- and high-yielding ones), and the model was then used to predict the yields of the new and mechanistically distinct MCRs described in the current publication. For the training set of the known MCRs, the Pearson correlation coefficient (ρ^2)

between the experimental and modeled yields was 0.80 with mean absolute error of 10.5. For the test set of reactions used in this study, ρ^2 = 0.86 and MAE = 7.3. These metrics compare quite favorably with generally unsatisfactory correlations observed for various machine learning models trained on "full" substrate-to-product reactions without any mechanistic knowledge[78-81].

Pre-curated collection of substrates available through Allchemy's user interface. Although arbitrary substrates can be input in Allchemy's MECH module, we have also curated a list of ~2200 simple and commercially available substrates that, in our experience, improve the chances of finding MCR reactions. To begin with, the Zinc collection[77] was pruned to retain only molecules with, at most, 15 heavy atoms. After removing stereochemistry, ~410,000 unique entries were left. Molecules containing either poorly reactive fragments (94 patterns, e.g., heterocycles, polycyclic systems, ethers) or several unfunctionalized carbon atoms were removed, as they only introduced unnecessary structural complexity without desired reactivity. The remaining molecules were queried for the presence of one or two reactive groups defined by experienced synthetic chemists (164 patterns of FGs listed in Supplementary **Table S2-S3**) – there were 36,294 such molecules of which 16,631 had one reactive FG and 19,663 had two reactive FGs. In the latter, we only kept molecules in which the FGs were separated by, at most, three atoms – in this way, when these molecules reacted, they were more likely to form smaller rings rather than macrocycles. For some FG combinations, there were many hits (e.g., the algorithm identified 97 commercially available isocyanates and 94 compounds possessing both aryl bromide and secondary amine FGs). In such cases, the compound with the lowest molecular mass was retained.

Correspondence

Correspondence and requests for materials should be directed to B.A.G. at nanogrzybowski@gmail.com

Acknowledgements

Development of the MECH module within the Allchemy platform (by R.R., A.W., K.M, T.K., B.M.-K., S.S., M.M., B.A.G.) was supported by internal funds of Allchemy, Inc. A.M., L.G., Y.B., P.G., O.P. gratefully acknowledge funding from the National Science Centre, Poland (Award 2018/30/A/ST5/00529). S.B. was supported by a grant from the Priority Research Area Anthropocene under the Strategic Programme Excellence Initiative at the Jagiellonian University. J. M. gratefully acknowledge funding from the Foundation for Polish Science (award TEAM/2017-4/38) – these three awards supported part of experimental validations described in this paper. Analysis of pathways and writing of the paper by B.A.G. was supported by the Institute for Basic Science, Korea (Project Code IBS-R020-D1).

Author contributions

R.R., A.W., K.M, S.S., M.M. and B.A.G. designed and developed Allchemy platform and performed analyses and calculations described in the paper. A.M. performed syntheses described in Figure 2, Y.B. and P.G. performed syntheses described in Figure 3a,b, B.M.-K. and T.K. performed syntheses described in Figure 3c,d, Y.B. performed syntheses described in Figure 3e,f, L.G. performed syntheses described in Figure 3g,h, O.P. performed syntheses described in Figure 4a with supervision from J.M., P.G. performed syntheses described in Figure 4c, S.B. performed

syntheses described in Extended Figure 6 with supervision from J.M. B.A.G. conceived and supervised research and wrote the paper with help from other authors.

Data availability

The full list of known MCRs and the interactive t-SNE map are deposited at https://mcrmap.allchemy.net. Networks for all examples described in the text are available for analysis at https://mcrchampionship.allchemy.net. All of these and any other desired searches can be performed at https://mech.allchemy.net. Results of MCR Championships are posted and updated at https://mcrchampionship.allchemy.net. User manuals are available in Supplementary **Section S1**. Multistep synthesis plans produced by Chematica/Synthia for targets made here via MCRs and one pots are deposited at https://zenodo.org/records/10817102 (note: no syntheses were found for Mach6 and for one of the two variants of Mach2).

Code availability

Interactive Allchemy MECH web-app is freely available at https://mech.allchemy.net (given server capacity, to five concurrent academic users on a rolling basis and two-week slots).

Competing interests

The authors declare the following competing interests: R.R., A.W., K.M, B.M.-K., T.K., S.S., M.M. and B.A.G. are consultants and/or stakeholders of Allchemy, Inc. Allchemy software and its MECH module is property of Allchemy Inc., USA. All queries about access options to Allchemy, including academic collaborations, should be sent to saraszymkuc@allchemy.net.

References

1. Roque, J. B., Kuroda, Y., Göttemann, L. T. & Sarpong, R. Deconstructive diversification of cyclic amines. *Nature* **564**, 244–248 (2018).

2. Kennedy, S. H., Dherange, B. D., Berger, K. J. & Levin M. D. Skeletal editing through direct nitrogen deletion of secondary amines. *Nature* **593**, 223–227 (2021).

3. Zhang, B. *et al.* Ni-electrocatalytic Csp3-Csp3 doubly decarboxylative coupling. *Nature* **606**, 313–318 (2022).

4. Ruffoni, A., Hampton, C., Simonetti, M. & Leonori, D. Photoexcited nitroarenes for the oxidative cleavage of alkenes. *Nature* **610**, 81–86 (2022).

5. Dömling, A. & Ugi, I. Multicomponent reactions with isocyanides. *Angew. Chem. Int. Ed.* **39**, 3168-3210 (2000).

6. Dömling, A., Wang, W. & Wang, K. Chemistry and biology of multicomponent reactions. *Chem. Rev.* **112**, 3083-3135 (2012).

7. Ganem, B. Strategies for innovation in multicomponent reaction design. *Acc. Chem. Res.* **42**, 463-472 (2009).

8. D'Souza, D. M. & Müller, T. J. J. Multi-component syntheses of heterocycles by transition-metal catalysis. *Chem. Soc. Rev.* **36**, 1095-1108 (2007).

9. Garbarino, S., Ravelli, D., Protti, S. & Basso, A. Photoinduced multicomponent reactions. *Angew. Chem. Int. Ed.* ***55***, 15476-15484 (2016).

10. Medley, J. W., & Movassaghi, M. Robinson's landmark synthesis of tropinone. *Chem. Comm.* **49**, 10775-10777 (2013).

11. Brandner, L. & Müller, T.J.J. Multicomponent synthesis of chromophores – The one-pot approach to functional π-systems. *Front. Chem.* **11**, 1124209 (2023).

12. Zhao, W. Y. & Chen, F. E. One-pot synthesis and its practical application in pharmaceutical industry. *Curr. Org. Synth.* **9**, 873-897 (2012).

13. Broadwater, S. J., Roth, S. L.; Price, K. E., Kobašlija, M. & McQuade, D. T. One-pot multi-step synthesis: a challenge spawning innovation. *Org. Biomol. Chem.* **3**, 2899-2906 (2005).

14. Wheeldon, I. *et al*. Substrate channeling as an approach to cascade reactions. *Nat. Chem.* **8**, 299-309 (2016).

15. Hayashi, Y. Time and pot economy in total synthesis. *Acc. Chem. Res.* **54**, 1385-1398 (2021).

16. Paul, B., Maji, M., Chakrabartia, K. & Kundu, S. Tandem transformations and multicomponent reactions utilizing alcohols following dehydrogenation strategy. *Org. Biomol. Chem.* **18**, 2193-2214 (2020).

17. Cioc, R. C., Ruijter, E. & Orru R. V. A. Multicomponent reactions: advanced tools for sustainable organic synthesis. *Green Chem.* **16**, 2958-2975 (2014).

18. Ruijter, E., Scheffelaar, R. & Orru, R. V. A. Multicomponent reaction design in the quest for molecular complexity and diversity. *Angew. Chem. Int. Ed.* **50**, 6234 – 6246 (2011).

19. Hayashi, H. *et al*. In silico reaction screening with difluorocarbene for *N*-difluoroalkylative dearomatization of pyridines. *Nat. Synth.* **1**, 804-814 (2022).

20. Novikov, M. S., Khlebnikov A. F., Krebs, A. & Kostikov, R. R. Unprecedented 1,3-dipolar cycloaddition of azomethine ylides derived from difluorocarbene and imines to carbonyl compounds − Synthesis of oxazolidine derivatives. *Eur. J. Org. Chem.* **1**, 133-137 (1998).

21. Dong, S., Fu, X. & Xu, X. [3+2]-Cycloaddition of catalytically generated pyridinium ylide: A general access to indolizine derivatives. *Asian J. Org. Chem.* **9**, 1133-1143 (2020).

22. Mikulak-Klucznik, B. *et al.* Computational planning of the synthesis of complex natural products. *Nature* **588**, 83–88 (2020).

23. Wołos, A. *et al.* Computer-designed repurposing of chemical wastes into drugs. *Nature* **604**, 668-676 (2022).

24. Lin, Y., Zhang, R., Wang, D. & Cernak, T. Computer-aided key step generation in alkaloid total synthesis. *Science* **379**, 453–457 (2023).

25. Wołos, A. *et al.*, Synthetic connectivity, emergence, and autocatalysis in the network of prebiotic chemistry. *Science* **369**, eaaw1955 (2020).

26. Gajewska, E. P. *et al.* Algorithmic discovery of tactical combinations for advanced organic syntheses. *Chem* **6**, 280–293 (2020).

27. Molga, K. *et al.* A computer algorithm to discover iterative sequences of organic reactions. *Nat. Synth.* **1**, 49–58 (2022).

28. Gothard, C. M. *et al*. Rewiring chemistry: algorithmic discovery and experimental validation of one-pot reactions in the network of organic chemistry. *Angew. Chem. Int. Ed.* **51**, 7922–7927 (2012).

29. Grossman, R. B. *The Art of Writing Reasonable Organic Reaction Mechanisms*. (Springer International Publishing, 2019).

30. Gund, T. M., Schleyer, P. R., Gund, P. H. & Wipke, W. T. Computer assisted graph theoretical analysis of complex mechanistic problems in polycyclic hydrocarbons. The mechanism of

diamantane formation from various pentacyclotetradecanes. *J. Am. Chem. Soc.* **97**, 743-751 (1975).

31. Marsili, M. *Computer chemistry.* (CRC Press, 1990).

32. Chen, J. H. & Baldi, P. No electron left behind: a rule-based expert system to predict chemical reactions and reaction mechanisms. *J. Chem. Inf. Model.* **49**, 2034-2043 (2009).

33. Kayala, M. A. & Baldi, P. ReactionPredictor: Prediction of complex chemical reactions at the mechanistic level using machine learning. *J. Chem. Inf. Model.* **51**, 2526-2540 (2012).

34. W. L. *et al*. CAMEO: a program for the logical prediction of the products of organic reactions. *Pure Appl. Chem.* **62**, 1921-1932 (1990).

35. Satoh, H. & Funatsu, K. SOPHIA, a knowledge base-guided reaction prediction system-utilization of a knowledge base derived from a reaction database. *J. Chem. Inf. Comput. Sci*. **35**, 34-44 (1995).

36. Patel S. C. and Burns N. Z. Conversion of aryl azides to aminopyridines. *J. Am. Chem. Soc.*, **144**, 17797–17802 (2022).

37. Guo, J. *et al.* An unexpected multi-component one-pot cascade reaction to access furanobenzodihydropyran-fused polycyclic heterocycles. *Chem. Commun.* **55**, 5207–5210 (2019).

38. Taitz, Y., Weininger, D. & Delany, J. J. Daylight Theory: SMARTS - A language for describing molecular patterns, https://www.daylight.com/dayhtml/doc/theory/theory.smarts.html (1997).

39. Molga, K., Gajewska, E. P., Szymkuć, S. & Grzybowski, B. A. The logic of translating chemical knowledge into machine-processable forms: a modern playground for physical-organic chemistry. *React. Chem. Eng.* **4**, 1506–1521 (2019).

40. Klucznik, T., Syntrivanis, LD., Baś, S. *et al.* Computational prediction of complex cationic rearrangement outcomes. *Nature* **625**, 508–515 (2024).

41. Roszak R., Beker W., Molga K. & Grzybowski B. A. Rapid and accurate prediction of pKa values of C−H Acids using graph convolutional neural networks. *J. Am. Chem. Soc.* **141**, 17142−17149 (2019).

42. Mayr, H.; Patz, M. Scales of nucleophilicity and electrophilicity: A system for ordering polar organic and organometallic reactions. *Angew. Chem. Int. Ed.* **33**, 938-957 (1994).

43. *Mayr's Database Of Reactivity Parameters - Start page* Available at: https://www.cup.lmu.de/oc/mayr/reaktionsdatenbank/. (Accessed: 6th December 2023)

44. Chavan, S. R. *et al.* Iminosugars spiro-linked with morpholine-fused 1,2,3-triazole: Synthesis, conformational analysis, glycosidase inhibitory activity, antifungal assay, and docking studies. *ACS Omega* **2**, 7203–7218 (2017).

45. Tanaka, N. *et al.* Isolation and structures of attenols A and B. Novel bicyclic triols from the Chinese bivalve *Pinna attenuata*. *Chem Lett* **28**, 1025–1026 (1999).

46. Chen, D. *et al.* Discovery, structural insight, and bioactivities of BY27 as a selective inhibitor of the second bromodomains of BET proteins. *Eur. J. Med. Chem.* **182**, 111633 (2019).

47. Teiji, K. *et al.* US2007219181A1 Multi-cyclic cinnamide derivatives. (2007).

48. Sikorski, W. H. & Reich, H. J. The Regioselectivity of addition of organolithium reagents to enones and enals: The role of HMPA. *J. Am. Chem. Soc.* **123**, 6527–6535 (2001).

49. Ireland R. E., Armstrong I., Lebreton J. D. J., Meissner R. S. & Rizzacasa M. A. Convergent synthesis of polyether ionophore antibiotics: synthesis of the spiroketal and tricyclic glycal segments of monensin. *J. Am. Chem. Soc.* **115**, 7152–7165 (1993).

50. Danishefsky, S. J., DeNinno, S. & Lartey, P. A concise and stereoselective route to the predominant stereochemical pattern of the tetrahydropyranoid antibiotics: an application to indanomycin. *J. Am. Chem. Soc*. **109**, 2082-2089 (1987).

51. Parker, K. A. & Georges, A. T. Reductive aromatization of quinols: synthesis of the C-arylglycoside nucleus of the papulacandins and chaetiacandin. *Org. Lett*. **2**, 497-499 (2000).

52. Gurjar, M. K., Krishna, L. M., Reddy, B. S. & Chorghade, M. S. A versatile approach to anti-asthmatic compound CMI-977 and its six-membered analogue. *Synthesis*, **2000**, 557-560 (2000).

53. Banwell, M. G. *et al.* Small molecule glycosaminoglycan mimetics. Patent WO 2006135973A1 (2006).

54. Mattson, R. J. & Catt, J. D. Piperazinyl-cyclohexanes and cyclohexenes. Patent US 6153611A (2000).

55. Chongquing, P., Zhu, Z., Zhang, M. & Gu, Z. Palladium-catalyzed enantioselective synthesis of 2-aryl cyclohex-2-enone atropisomers: platform molecules for the divergent synthesis of axially chiral biaryl compounds. *Angew. Chem. Int. Ed.* **56**, 4777-4781 (2017).

56. Mahecha-Mahecha, C. *et al.* Sequential Suzuki−Miyaura coupling/Lewis acid-catalyzed cyclization: an entry to functionalized cycloalkane-fused naphthalenes. *Org. Lett.* **22**, 6267-6271 (2020).

57. Xu, W. & Yoshikai, N. Cobalt-catalyzed directed C–H alkenylation of pivalophenone N–H imine with alkenyl phosphates. *Beilstein J. Org. Chem*. **14**, 709-715 (2018).

58. Kang, D., Kim, J., Oh, S. & Lee, P. H. Synthesis of naphthalenes via platinum-catalyzed hydroarylation of aryl enynes. *Org. Lett.* **14**, 5636–5639 (2012).

59. Zhang, X., Sarkar, S. & Larock, R. C. Synthesis of naphthalenes and 2-naphthols by the electrophilic cyclization of alkynes. *J. Org. Chem.* **71**, 236-243 (2006).

60. Mohan, C., Singh, P., & Mahajan, M. P. Facile synthesis and regioselective thio-Claisen rearrangements of 5-prop-2-ynyl/enyl-sulfanyl pyrimidinones: transformation to thienopyrimidinones. *Tetrahedron* **61**, 10774-10780 (2005).

61. Kumar, S. V. *et al.* Cyclocondensation of arylhydrazines with 1, 3-bis (het) arylmonothio-1, 3-diketones and 1, 3-bis (het) aryl-3-(methylthio)-2-propenones: Synthesis of 1-aryl-3, 5-bis (het) arylpyrazoles with complementary regioselectivity. *J. Org. Chem*. **78**, 4960-4973 (2013).

62. Splivallo, R., & Ebeler, S. E. Sulfur volatiles of microbial origin are key contributors to human-sensed truffle aroma. *Appl. Microbiol. Biotechnol.* **99**, 2583-2592 (2015).

63. Dai J., Krohn K., Gehle D., Kock I., Flörke U., Aust H. J. & Rheinheimer J. New oblongolides isolated from the endophytic fungus Phomopsis sp. from Melilotus dentata from the shores of the Baltic Sea. *Eur. J. Org. Chem.* **2005**, 4009-4016 (2005).

64. Bunyapaiboonsri T., Yoiprommarat S., Srikitikulchai P., Srichomthong K., & Lumyong S. Oblongolides from the Endophytic Fungus Phomopsis sp. BCC 9789. *J. Nat. Prod.* **73**, 55-59 (2010).

65. Shing T.K.M. & Yang J. A short synthesis of natural (-)-oblongolide via an intramolecular or a transannular Diels-Alder reaction. *J. Org. Chem.* **60**, 5785-5789 (1995).

66. I. V. Magedov *et al.* Reengineered epipodophyllotoxin. *Chem. Commun.* **48**, 10416-10418 (2012).

67. Hur, J., Jang, J. & Sim, J. A Review of the pharmacological activities and recent synthetic advances of γ-butyrolactones. *Int. J. Mol. Sci.* **22**, (2021).

68. Le, H. V. *et al.* Design and mechanism of tetrahydrothiophene-based γ-aminobutyric acid aminotransferase inactivators. *J. Am. Chem. Soc.* **137**, 4525–4533 (2015).

69. Kalashnikov, A. I., Sysolyatin, S. V., Sakovich, G. V., Sonina, E. G. & Shchurova, I. A. Facile method for the synthesis of oseltamivir phosphate. *Russ. Chem. Bull.* **62**, 163–170 (2013).

70. Tavakoli, M., Chiu, Y. T. T., Baldi, P., Carlton, A. M. & Van Vranken, D. RMechDB: A public database of elementary radical reaction steps. *J. Chem. Inf. Model.* **63**, 1114–1123 (2023).

71. Tavakoli, H.R., Moosavi, S.M. & Bazgir, A. $ZrOCl_2 \cdot 8H_2O$ as an efficient catalyst for the synthesis of dibenzo [*b*,*i*]xanthene-tetraones and fluorescent hydroxyl naphthalene-1,4-diones. *Res. Chem. Intermed*. **41**, 3041–3046 (2015).

72. Liu, D., Zhou, S. & Gao, J. Room-temperature synthesis of hydroxylnaphthalene-1,4-dione derivative catalyzed by phenylphosphinic acid, *Synth. Commun.* **44**, 1286-1290 (2014).

73. Shaabani, S. Naimi-Jama, M.R. & Maleki, A. Synthesis of 2-hydroxy-1,4-naphthoquinone derivatives via a three-component reaction catalyzed by nanoporous MCM-41, *Dyes Pigm.* **122**, 46-49 (2015).

74. Shaterian, H.R. & Mohammadnia, M. Effective preparation of 2-amino-3-cyano-4-aryl-5,10-dioxo-5,10-dihydro-4H-benzo[g]chromene and hydroxyl naphthalene-1,4-dione derivatives under ambient and solvent-free conditions. *J. Mol. Liq.* **177**, 353-360 (2013).

75. Tayama, E., Sato, R., Takedachi, K., Iwamoto, H. Hasegawa, E. A formal method for the de-N,N-dialkylation of Sommelet–Hauser rearrangement products. *Tetrahedron* **68**, 4710-4718 (2012).

76. Kim, S.H. Lee, H.S., Kim, K.H. & Kim, J.N. An expedient synthesis of poly-substituted 1-arylisoquinolines from δ-ketonitriles via indium-mediated Barbier reaction protocol. *Tetrahedron Lett.* **50**, 6476-6479 (2009).

77. Irwin, J. J., & Shoichet, B. K. ZINC − A Free database of commercially available compounds for virtual screening. *J. Chem. Inf. Model.*, **45**, 177–182 (2005).

78. Saebi, M., Nan, B., Herr, J.E. *et al.* On the use of real-world datasets for reaction yield prediction. *Chem. Sci.* **14**, 4997-5005 (2023).

79. Liu, Z., Moroz, Y.S., Isayev, O. The challenge of balancing model sensitivity and robustness in predicting yields: a benchmarking study of amide coupling reactions. *Chem. Sci.* **14**, 10835-10846 (2023).

80. Beker, W., Roszak, R., Wolos, A. *et al.* Machine learning may sometimes simply capture literature popularity trends: A case study of heterocyclic Suzuki-Miyaura coupling, *J. Am. Chem. Soc.*, **144**, 4819–4827 (2022).

81. Skoraczyński, G., Dittwald, P., Miasojedow, B. *et al.* Predicting the outcomes of organic reactions via machine learning: are current descriptors sufficient? *Sci. Rep.* **7**, 3582 (2017).

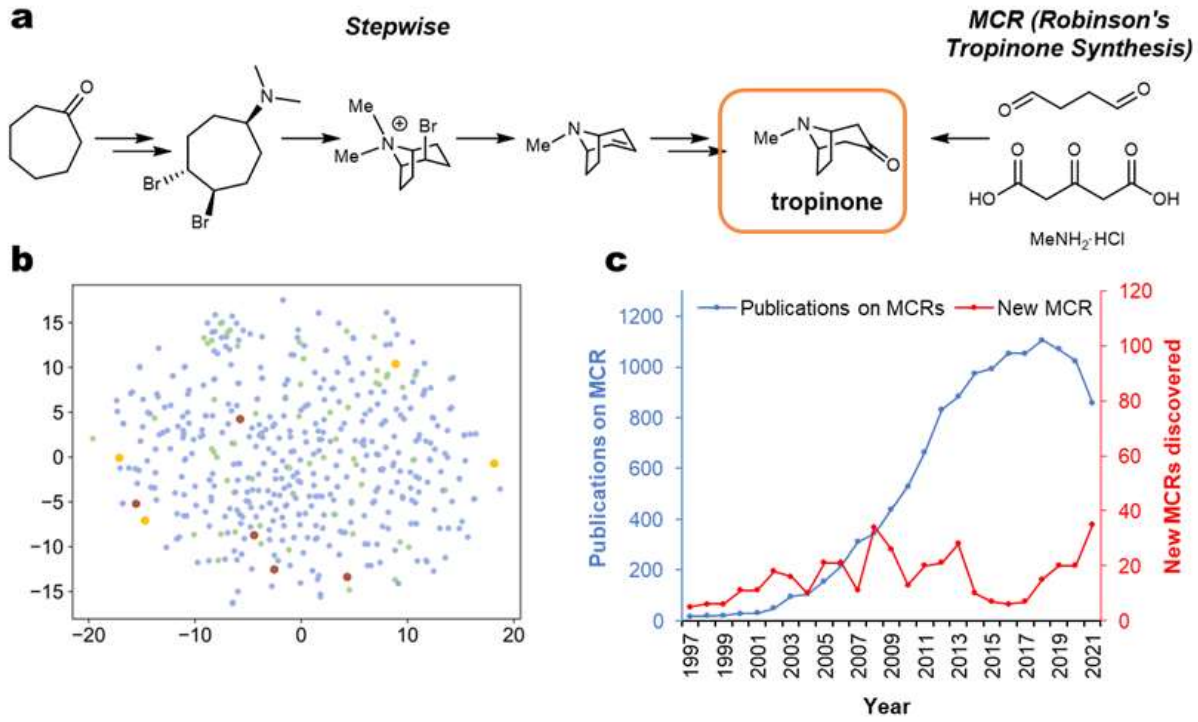

Figure 1 | Significance and current discovery rate of multicomponent reactions. a, A classic example illustrating the elegance and efficiency of Robinson's one-step, MCR synthesis of tropinone vs. prior, fifteen-step synthesis[10]. In the latter, only two key steps are shown. **b,** t-SNE projection "map" illustrating diversity of 422 known MCR (smaller *blue* markers) and 63 one-pot classes (*green*) vs. the new MCRs and one-pots (larger *red* and *yellow* markers, respectively) described in this work and validated by experiment. The full list of known MCRs and the interactive t-SNE map are deposited at https://mcrmap.allchemy.net. **c,** Blue line and left axis quantify the numbers of papers on MCRs published in a given year (based on "multicomponent reaction" query of the Web of Knowledge database, October 2022). Red line and right axis plot the numbers of new MCRs reported in a given year. This analysis is based on the extensive literature review counting unique reaction types (i.e., not different precedents of the same MCR). The dataset is posted at https://zenodo.org/records/10817102.

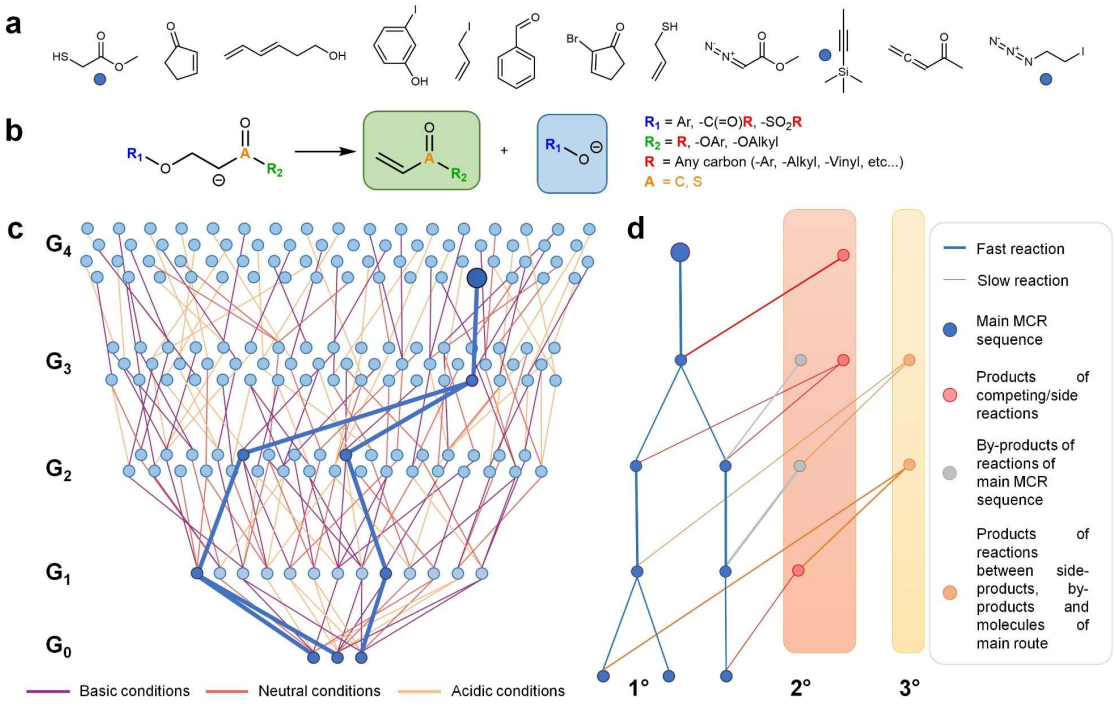

Figure 2 | Key elements of the MECH algorithm to discover new MCRs. a, Examples of simple starting materials from the collection of 2200 (see main text and **Methods**). **b,** Abbreviated example of one of ~8000 mechanistic transforms, here E1cB elimination. Different positions can accommodate various substituents, some of which are listed to the right of the reaction scheme. Note that the transform is coded to account for the by-product(s), here a phenoxide, carboxylate or mesylate. Classification of reaction conditions, rates, etc., are also parts of the transform's record but, for clarity, are not shown here. **c,** Application of mechanistic transforms to a given set of starting materials iteratively expands the synthetic generations, G_n, of a network of possible intermediates and immediate by-products. In the schematic miniature drawn, the three circle markers in the bottom row (G_0) may be the three molecules from panel (a), and the network is expanded to G_4. Different colors of connections between the nodes are intended to denote different types of conditions – to emphasize that this "forward" network expansion probes all conditions' combinations. Within the network thus constructed, the conditions may be matching (i.e., mutually

compatible), corresponding to a MCR candidate at the Level 1 of analysis (sequence of steps highlighted in *dark blue*). **d,** Such a sequence is expended "sideways", to perform analyses at Levels 2 and higher. Level 2 – "branching-out" of the main path to include by-products (*grey*) and products of competing/side reactions possible under the same class of reaction conditions (*red*; for condition types, see **Methods**); Level 3 – further branching to account for the reactions between side- and by-products. At Level 3 (and higher, not shown here for clarity but see **Figure 3b**), undesired reactions of side-/by-products with each other and with the members of the main pathway are also considered and marked in *orange*. Faster reactions are represented schematically by thicker connections and it is essential that, at any junction, the side reactions are not faster that the main-path ones.

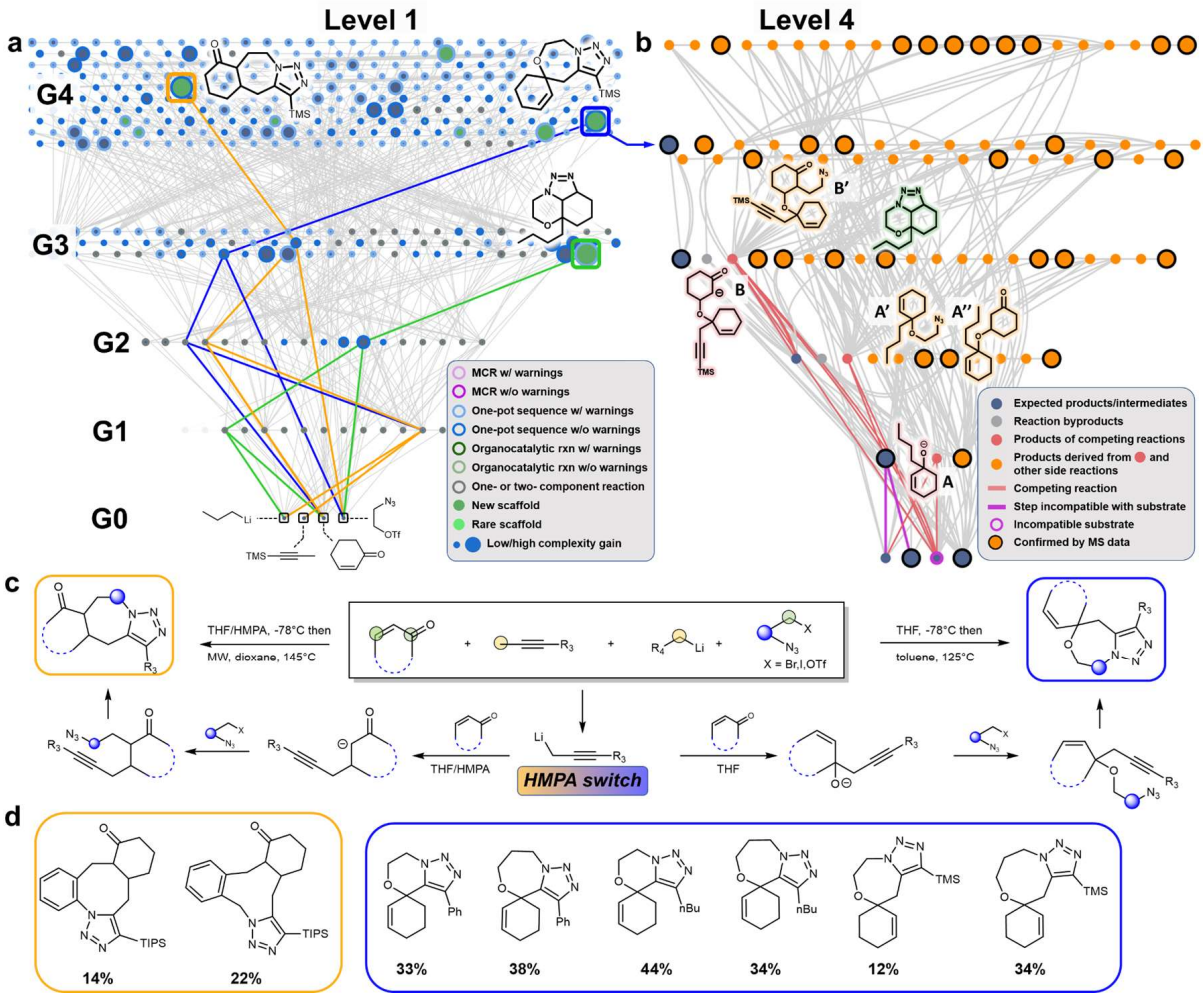

Figure 3 | Example of newly-discovered one-pot sequences and the corresponding mechanistic network expanded to Level 4, L4. a, Screenshot of Level 1, L1 network propagated from cyclohexenone, trimethylsilylpropyne, *n*-butyllithium and azidotriflate substrates to n = 4 generations, G_4. The network encompasses all mutually-compatible sequences possible under different types of conditions. Node sizes are proportional to complexity increase per mechanistic step, ΔC/n (cf. **Methods**). Colors of the halos define MCR/one-pot sequences with or without warnings. Nodes whose interiors are colored *green* correspond to scaffolds not described in the literature. Within this network, two sequences (traced in *blue* and *orange*) up to G_4 are predicted to be one-pot without warnings and leading to new scaffolds offering marked increase in ΔC/n

(largest *green* nodes). A path to another complex scaffold in G_3 is also marked (in *green*). This product is predicted to form from the 1,2-adduct of nBuLi/cyclohexanone/azide cyclizing onto the double bond, and was detected by ESI-MS in the reaction mixture (structure highlighted in *green* in the L4 network in panel (b)). **b,** Screenshot of the network branched-out from the blue pathway in (a) and analyzed at Level 4 (for networks analyzed at Levels 2 and 3, see **Extended Figure 1;** interactive network expandable to L4 is deposited at https://mcrchampionship.allchemy.net). This L4 network encompasses various by- and side-products (*grey* and *red* nodes, respectively) and their further reactions (products marked in *orange*) between themselves and with the "parent" pathway. Larger orange nodes are likely structural assignments of peaks observed in the ESI-MS of the crude-reaction mixture. Interestingly, although the peaks corresponding to some predicted byproducts (e.g., ***A***, ***B***; structures drawn here with *pink* highlights) were not manifest in the ESI-MS spectra, their formation is corroborated by further products (***A'***, ***A''***, ***B'***; structures drawn with *orange* highlights) that can only be derived from these undetected species. For more structural assignments, see **Extended Figure 1**. Also, the key cross-reactivity mandating sequential addition of reagents rather than MCR (i.e., reaction of alkyllithium with enone during metalation of alkyne) is highlighted by *brighter pink* connections at the bottom of the network, **c,** General scheme and intermediates of the *blue* and *orange* one-pot pathways (from (a)) along with reaction conditions. In the substrates, the available nucleophilic and electrophilic sites are marked yellow and green, respectively, while the dark blue circle and the dotted arcs denote linkers between the azide and (pseudo)halides and a cyclic or acyclic fragment of the enone, respectively. The regioselectivity of addition (1,2- vs 1,4-) of propargyllithium reagent is controlled by the addition of HMPA as co-solvent. **d,** Specific molecules synthesized according to the general protocol along with the

corresponding isolated yields. Note that the yields are low, as indeed predicted by the algorithm (see main text).

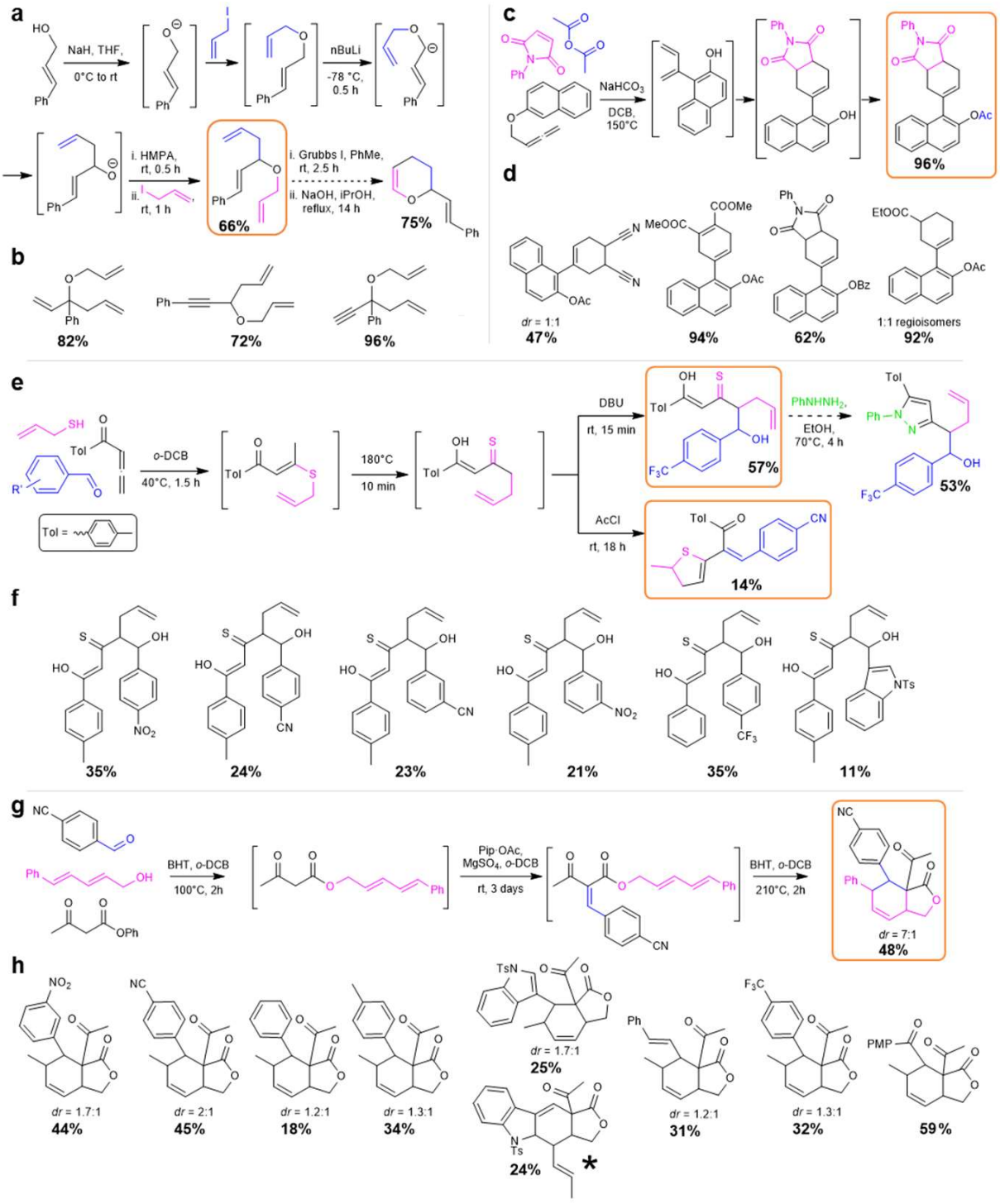

Figure 4 | Computer-discovered one-pot sequences and MCRs. For details of mechanistic networks, see **Extended Figures 2-5**. **a,** Scheme of a one-pot sequence for the synthesis of

branched allyl ethers. The sequence is detected as one-pot rather than the MCR because excessive allyl iodide would react with *n*-butyllithium, hampering deprotonation and subsequent Wittig rearrangement (cf. **Extended Figure 2b** marking this conflict). Non-isolated intermediates are shown in brackets and the isolated product is framed in *orange*. This product has been separately cyclized via ring-closing metathesis to afford cyclic enol ether. **b,** Additional derivatives prepared by the one-pot method from (a) using as substrates allyl iodide and commercially available β,γ-unsaturated alcohols. **c**, Scheme of a MCR producing unsaturated β-naphthol esters. Key non-isolated intermediates are shown in brackets and the isolated product is framed in *orange*. **d**, Additional derivatives prepared by this MCR from (c) using different commercially available dienophiles and acylating agents. **e,** Scheme of a MCR producing unsaturated hydroxylated monothio-β-diketones (existing in the thioenol tautomeric form) under basic conditions (*top*) or 2,3-dihydrothiophenes under acidic conditions (*bottom*) applied during the last step. Non-isolated intermediates are shown in brackets and the isolated products (originally predicted for the *top* MCR and highest yielding for the *bottom* one are framed in *orange*. The monothio-β-diketone product has been separately reacted (*dashed* arrow) with phenylhydrazine (*green*) to afford a substituted pyrazole. **f**, Additional products prepared by the *top* MCR from (**e**). **g**, Scheme of the MCR producing unsaturated bicyclic lactones. Key non-isolated intermediates are shown in brackets and the isolated product is framed in *orange*. **h**, Additional derivatives prepared by a MCR from (g) using different commercially available aldehydes and dienes. Abbreviations: BHT, butylhydroxytoluene; DCB, dichlorobenzene; THF, tetrahydrofuran; DBU, 1,8-diazabicyclo(5.4.0)undec-7-ene; Pip·OAc, piperidinium acetate; dr, diastereomeric ratio. The product of reverse-demand Diels-Alder cyclization is marked with a star. Percentage values in all panels are isolated yields.

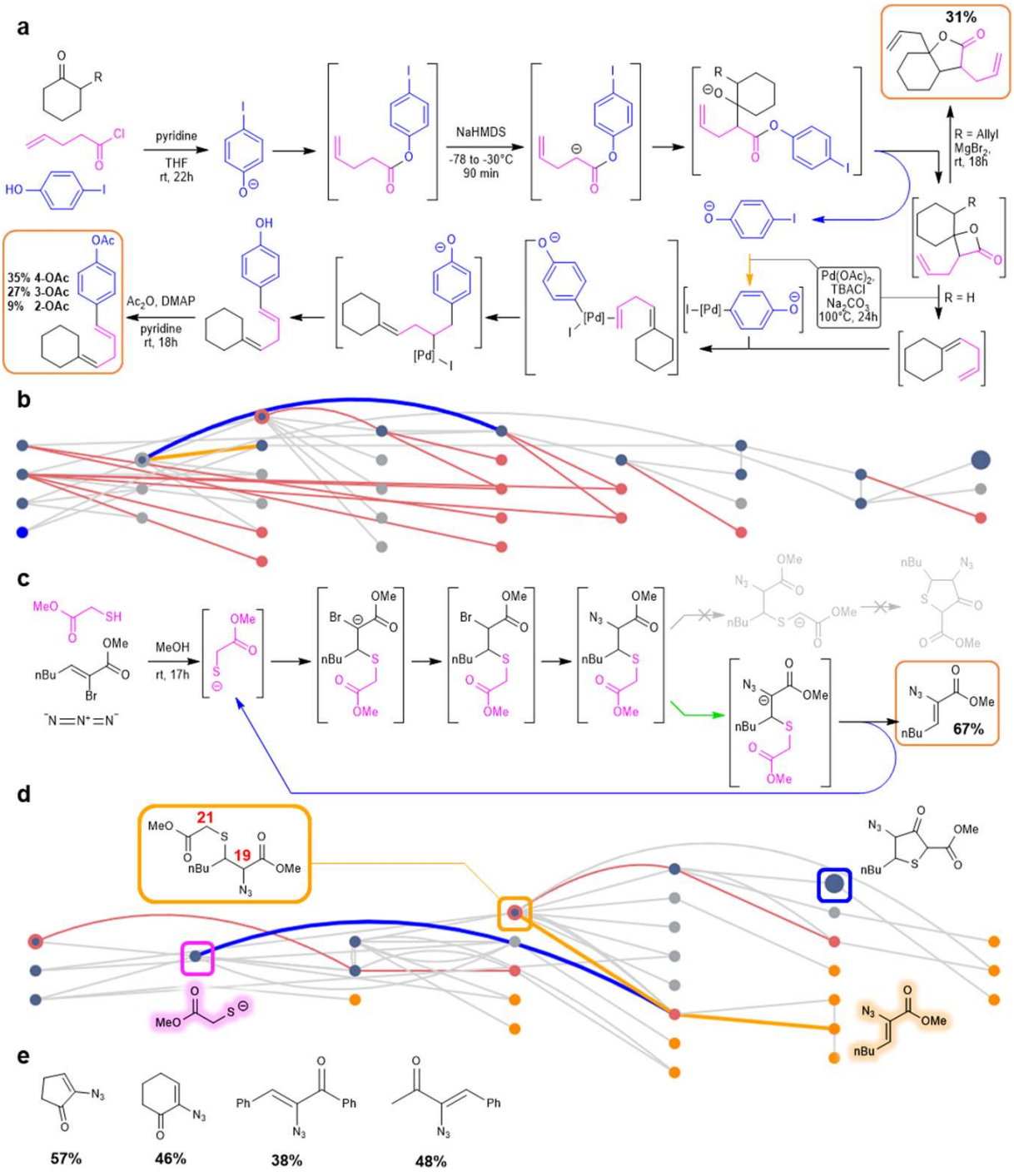

Figure 5 | Computer-discovered substrate-reusing MCRs and an organocatalytic reaction. a, Scheme of a MCR for the synthesis of arylated skipped dienes. Non-isolated intermediates are shown in brackets and the isolated products are framed in *orange*. The obtained dienes were

separately acetylated for the purpose of purification. The bicyclic lactone (*upper right*) was obtained from substituted cyclohexanone (R = allyl) and phenol substrates when $MgBr \cdot Et_2O$ was used instead of the Pd-catalyst. **b,** The L3 graph view of the path leading to the arylated diene from (a). Reuse of iodophenol byproduct in Heck-coupling (with oxidative addition step marked *orange*) is marked with the *blue* arc. **c,** Scheme of organocatalytic thiol-catalyzed sp^2-azidation. Non-isolated intermediates are shown in brackets and the isolated products are framed in *orange*. **d,** The L2 graph view of the path from (c). Reuse of thiol, acting as an organocatalyst, is marked with the *blue* arc. **e,** Additional vinyl azides prepared by the MCR from (c) using different α-bromoenones.

Extended Figures.

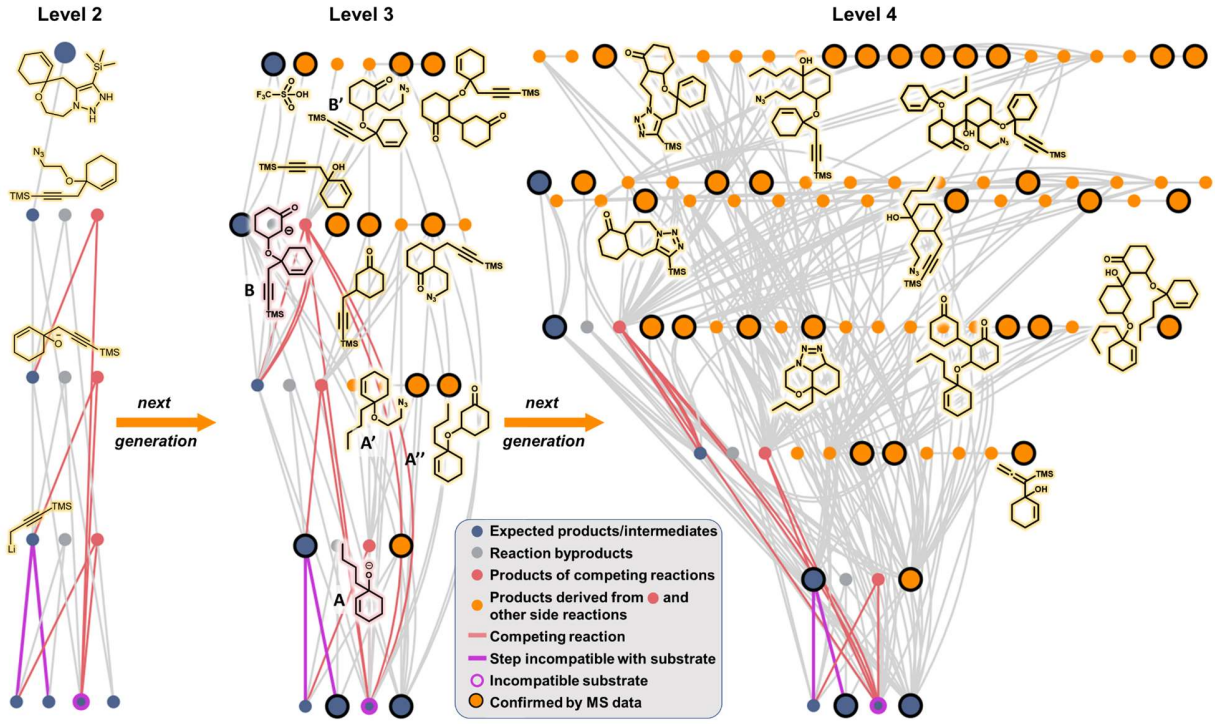

Extended Figure 1 | Different levels of analysis and additional ESI-MS assignments for the spirocyclic triazole path from Figure 3. Allchemy MECH module screenshots of networks at Levels 2,3,4 with larger orange nodes denoting likely structural assignments (overlaid as highlighted structures, in addition to structures already shown in **Figure 3b**) of peaks observed in the ESI-MS of the crude-reaction mixture.

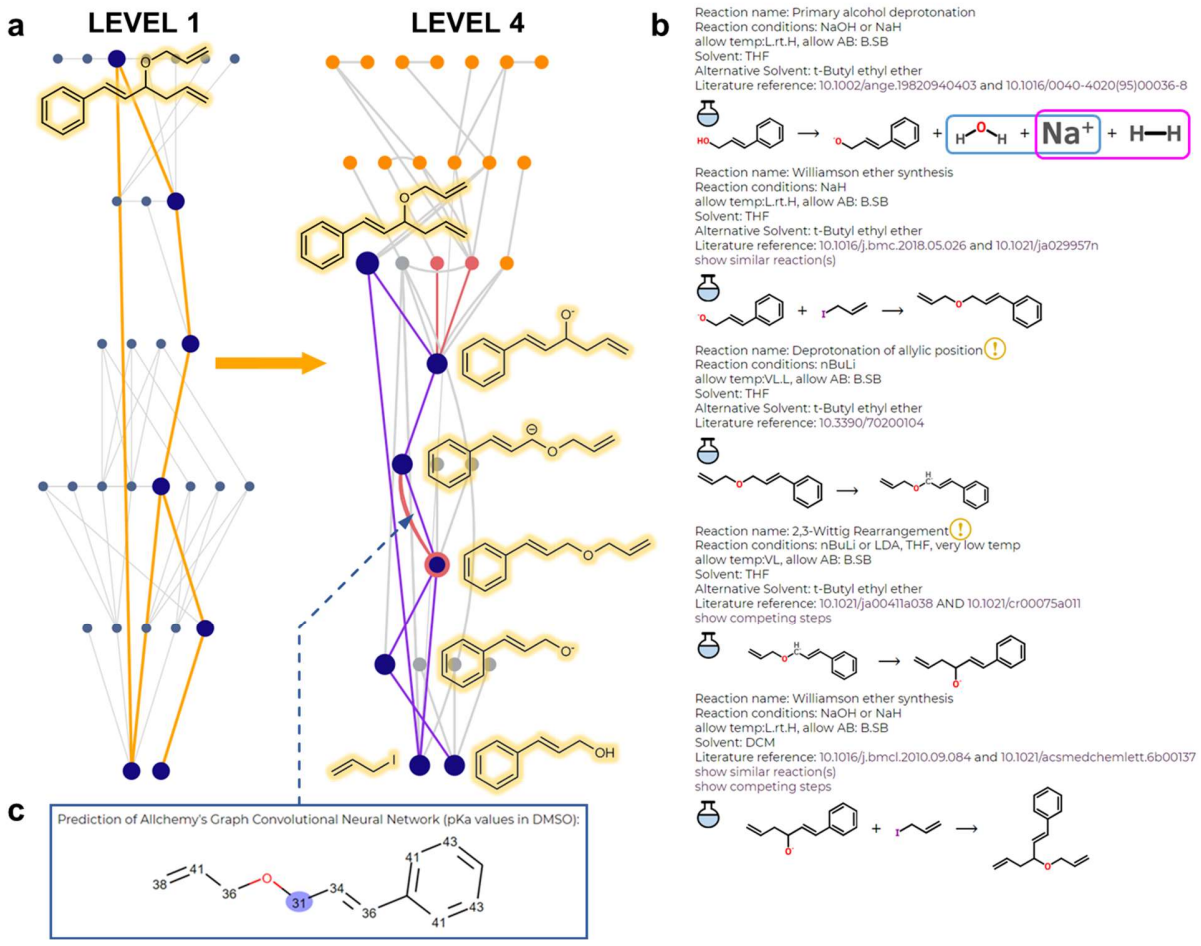

Extended Figure 2 | One-pot sequence from Figure 4a, starting from allyl iodide and cinnamyl alcohol. The sequence is presented as **a,** Level 1 and Level 4 networks and, **b,** list of mechanistic steps (both networks and the list are screenshots from Allchemy's MECH module). Every step is accompanied by name, typical reaction conditions, solvent, and hyperlinks to illustrative literature references. Another hyperlink allows visualizing competing reactions whereas clicking the "flask" icon expands a given step to show its byproducts (here, for deprotonation of primary alcohols step, indicated by blue and pink frames, corresponding to alternative reagents for this reaction). The exclamation mark points to the key cross-reactivity conflict which renders this sequence one-pot rather than MCR (excessive allyl iodide would react

with *n*-butyllithium, hampering deprotonation and subsequent Witting rearrangement. **c,** Allchemy's pKa filter[41] predicting correctly the most acidic CH position in the deprotonation step.

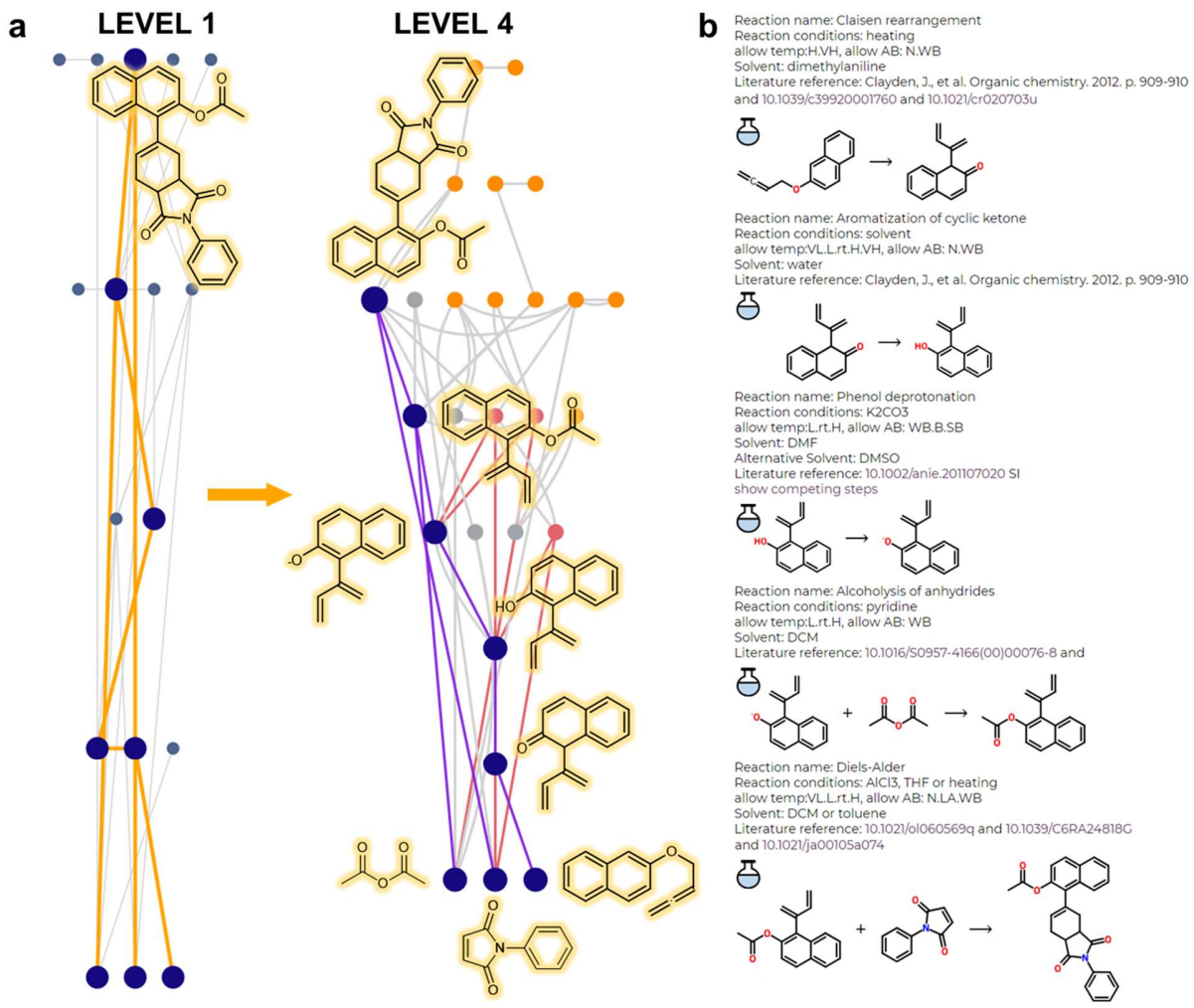

Extended Figure 3 | Multicomponent reaction from Figure 4c, starting from 2-(buta-2,3-dien-1-yloxy)naphthalene, *N*-phenylmaleimide and acetic anhydride. This MCR is presented here as **a,** Level 1 and Level 4 networks and **b,** list of mechanistic steps (both networks and the list are screenshots from Allchemy's MECH module). Every step is accompanied by name, typical reaction conditions, solvent, and hyperlinks to illustrative literature references. As in Extended Figure 2, by-products of each reaction can be visualized by clicking on the "flask" icon.

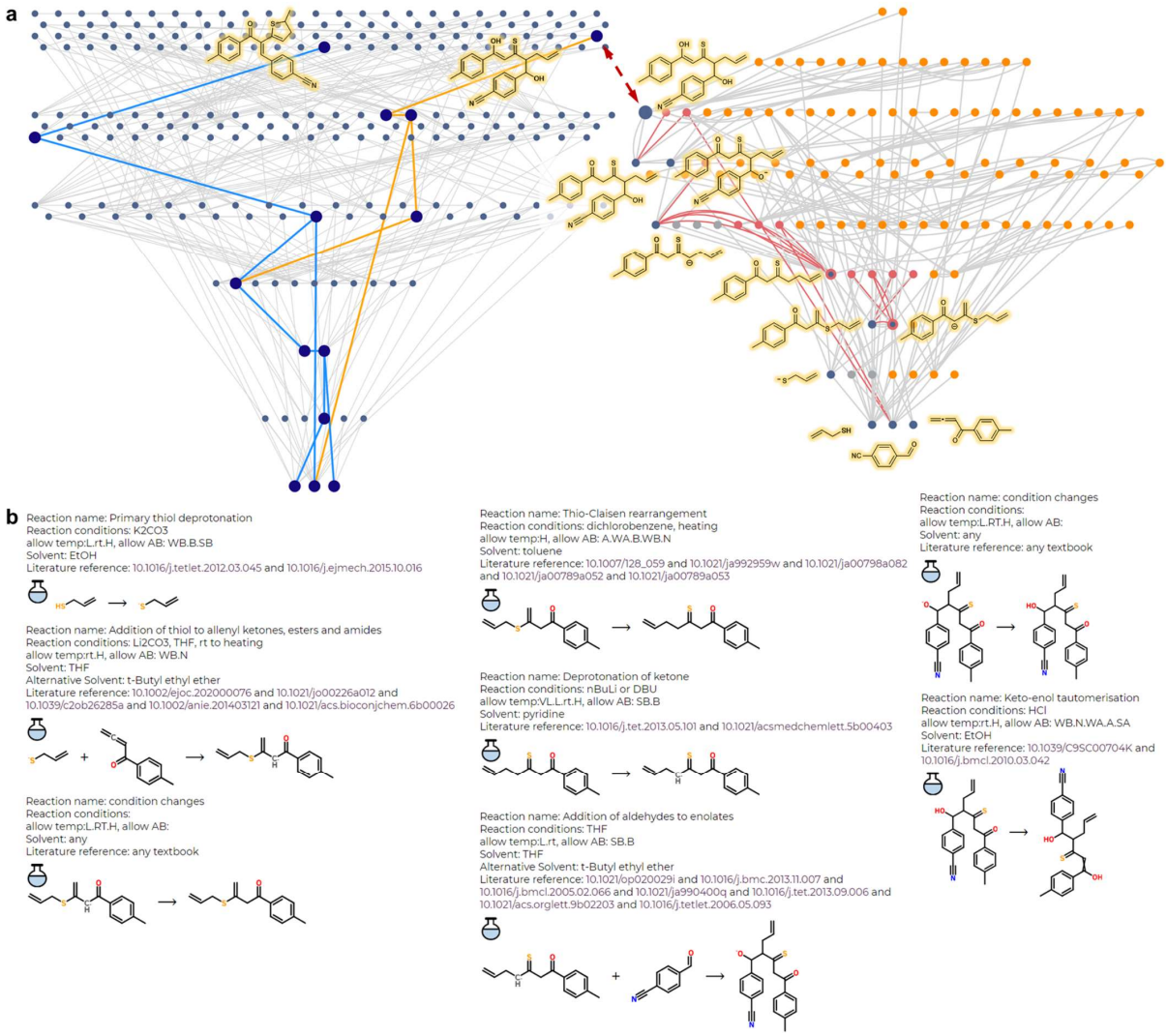

Extended Figure 4 | The first of the two MCRs from Figure 4e, starting from allyl thiol, 4-cyanobenzaldehyde and 1-(p-tolyl)buta-2,3-dien-1-one, catalyzed by DBU. This MCR is presented here as **a,** Level 1 and Level 4 networks and, **b,** list of mechanistic steps (both networks and the list are screenshots from Allchemy's MECH module). Every step is accompanied by name, typical reaction conditions, solvent, and hyperlinks to illustrative literature references. As in Extended Figure 2, by-products of each reaction can be visualized by clicking on the "flask" icon.

In Level 4 network, terminal nodes corresponding to unstable molecules (charged, enols) that were not involved in any further reactions are not shown for clarity.

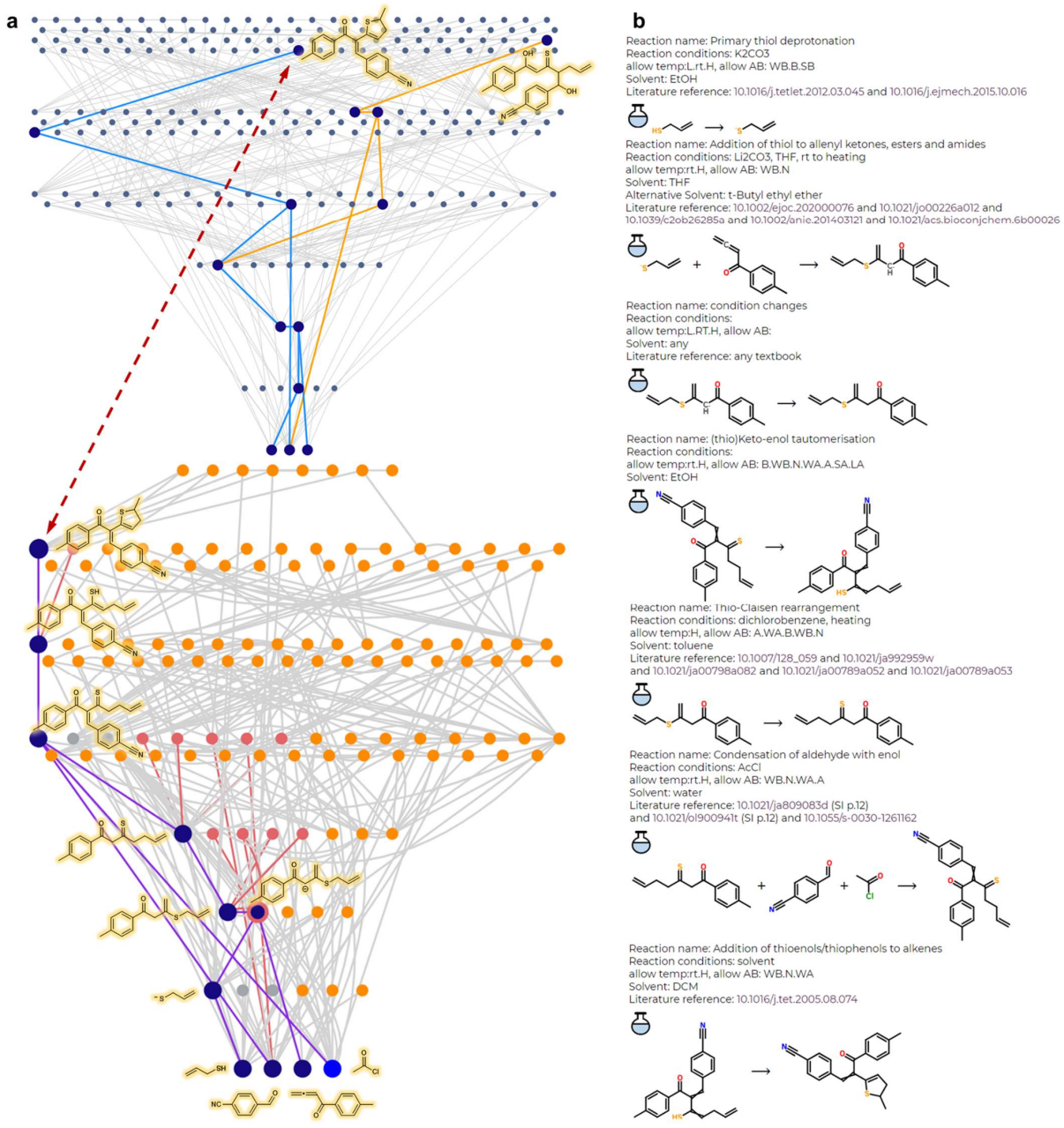

Extended Figure 5 | The second MCR from Figure 4e, starting from allyl thiol, 4-cyanobenzaldehyde and 1-(p-tolyl)buta-2,3-dien-1-one, catalyzed by acyl chloride. This MCR is presented here as **a,** Level 1 and Level 4 networks and, **b,** list of mechanistic steps (both networks

and the list are screenshots from Allchemy's MECH module). Every step is accompanied by name, typical reaction conditions, solvent, and hyperlinks to illustrative literature references. As in Extended Figure 2, by-products of each reaction can be visualized by clicking on the "flask" icon. In Level 4 network, terminal nodes corresponding to unstable molecules (charged, enols) that were not involved in any further reactions are not shown for clarity.

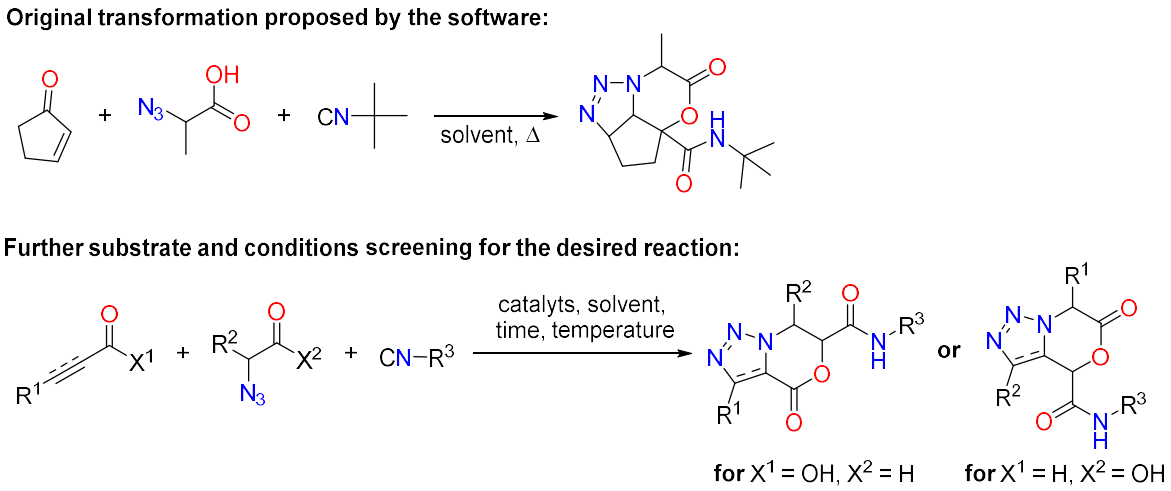

Extended Figure 6 | Example of a failed reaction. Top part shows the MECH-proposed MCR which was of some interest to us due to it combining a known Passerini MCR with a [3+2] cycloaddition of azide and alkene. This MCR was expected to result in a tricyclic structure containing 4,5-dihydro-triazole and lactone rings. In experimental validation, various combinations of substrates were investigated, e.g., 2-cyclopentene-1-one which was unreactive, cinnamaldehyde and aliphatic/aromatic azido acids resulting only in Passerini products with moderate to good yields, or cinnamic acid with aliphatic/aromatic azido-aldehydes (with similar effect). Using alkynes as well-recognized substrates for Huisgen cycloaddition (*bottom* scheme) did not solve the problem. Neither acids nor aldehydes bearing triple bonds in their structures led, in the presence of copper or ruthenium catalyst, to desired products. Literature investigation (*Chem. Rev.* 116, 14726, **2016**; *J. Org. Chem.* 71, 8680, **2006**; *J. Am. Chem. Soc.*,132, 41, 14327, **2010**) and analysis of conformation energies of theoretical products suggest that desired regioselectivity of cycloaddition in all investigated examples would entail formation of prohibitively strained structures. This failed example points to the need to constantly improve our static library of problematic motifs or even replace it with on-the-fly calculations by molecular

mechanics (which, as we showed in recent work on carbocationic rearrangements, is doable[40] but increases CPU time considerably).

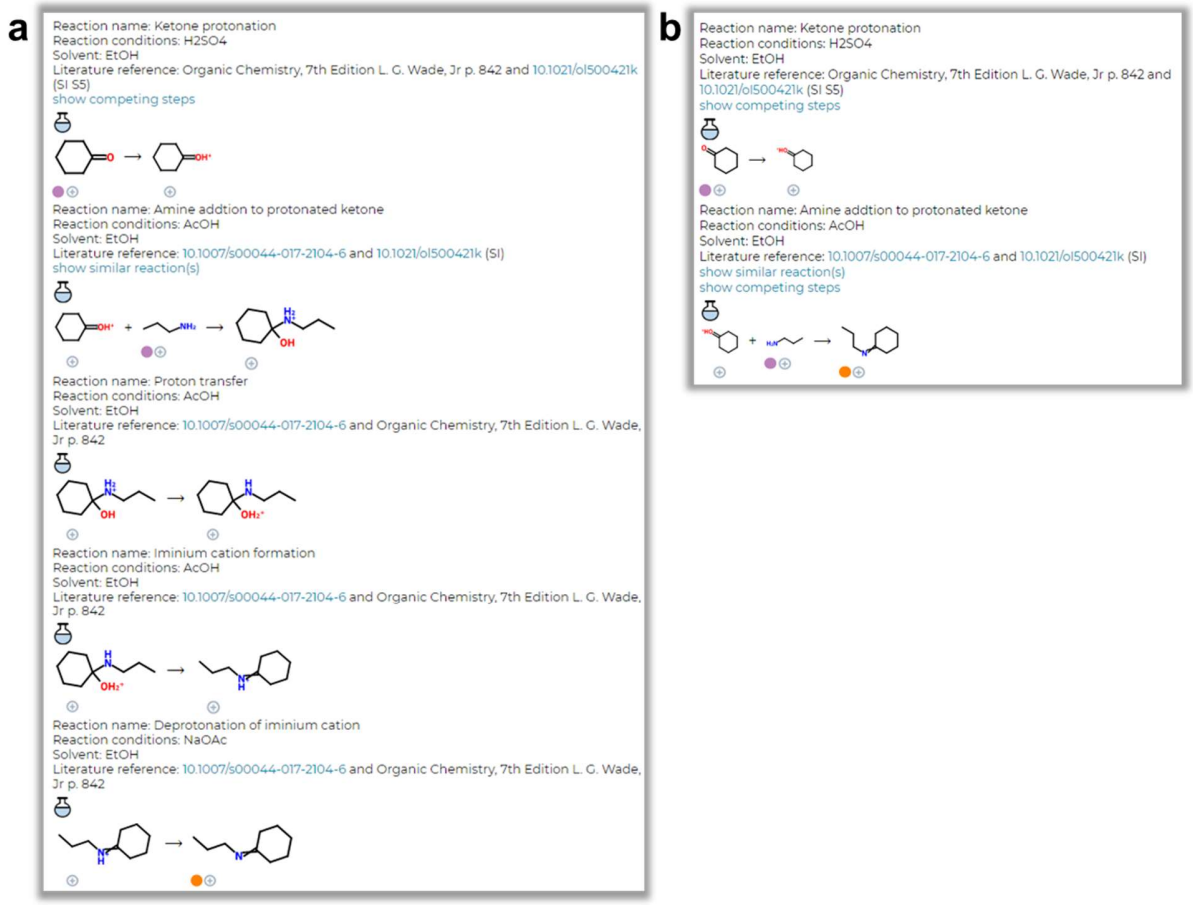

Extended Figure 7 | Individual mechanistic steps vs. "supersteps". Allchemy screenshots illustrating **a,** Imine formation divided into all mechanistic steps; and **b,** Imine formation with "short-cut" combining *Amine addition to protonated ketone*, *Proton transfer*, *Iminium cation formation* and *Deprotonation of iminium cation* into one "superstep".